

# Journal of Visualized Experiments

## 2D and 3D echocardiography in the axolotl (*Ambystoma mexicanum*)

--Manuscript Draft--

<b>Manuscript Number:</b>	JoVE57089R1
<b>Full Title:</b>	2D and 3D echocardiography in the axolotl ( <i>Ambystoma mexicanum</i> )
<b>Article Type:</b>	Invited Methods Article - JoVE Produced Video
<b>Keywords:</b>	Echocardiography; ultrasound; heart; cardiac ultrasonography; regeneration; axolotl; <i>Ambystoma mexicanum</i> ; spatio-temporal image correlation
<b>Manuscript Classifications:</b>	1.7.541: Heart; 2.1.50.150.900.90: Amphibians; 2.1.50.150.900.90.608.80.68: <i>Ambystoma</i> ; 3.14.280.647.500: Myocardial Infarction; 5.1.370.350.130: Cardiac Imaging Techniques; 5.1.370.350.130.750: Echocardiography; 5.1.370.350.400.200: Echocardiography, Three-Dimensional; 5.1.370.350.850: Ultrasonography
<b>Corresponding Author:</b>	Henrik Lauridsen, PhD Aarhus Universitet Aarhus N, NA DENMARK
<b>Corresponding Author Secondary Information:</b>	
<b>Corresponding Author E-Mail:</b>	henrik@clin.au.dk
<b>Corresponding Author's Institution:</b>	Aarhus Universitet
<b>Corresponding Author's Secondary Institution:</b>	
<b>First Author:</b>	Anita Dittrich
<b>First Author Secondary Information:</b>	
<b>Other Authors:</b>	Anita Dittrich Mathias Møller Thygesen
<b>Order of Authors Secondary Information:</b>	
<b>Abstract:</b>	Cardiac malfunction as a result of ischemic heart disease is a major challenge, and regenerative therapies to the heart are in high demand. A few model species such as zebrafish and salamanders that are capable of intrinsic heart regeneration hold promise for future regenerative therapies for human patients. To evaluate the outcome of cardioregenerative experiments it is imperative that heart function can be monitored. The axolotl salamander ( <i>Ambystoma mexicanum</i> ) represents a well-established model species in regenerative biology attaining sizes that allows for evaluation of cardiac function. The purpose of this protocol is to establish methods to reproducibly measure cardiac function in the axolotl using echocardiography. The application of different anesthetics (benzocaine, MS-222, and propofol) is demonstrated, and the acquisition of two-dimensional echocardiographic data in both anesthetized and unanesthetized axolotls is described. Two-dimensional echocardiography of the three-dimensional heart can suffer from imprecision and subjectivity of measurements, and to alleviate this phenomenon a solid method, namely intra/inter-operator/observer analysis, to measure and minimize this bias is demonstrated. Finally, a method to acquire three-dimensional echocardiographic data of the beating axolotl heart at a very high spatiotemporal resolution and with pronounced blood-to-tissue contrast is described. Overall, this protocol should provide the necessary methods to evaluate cardiac function and model anatomy and flow dynamics in the axolotl using ultrasound imaging with applications in both regenerative biology and general physiological experiments.
<b>Author Comments:</b>	In addition to several figures featuring echocardiographic data we have produced several videos displaying the same data. It is our experience that echocardiographic data is best displayed as a combination between annotated figures and playing videos. Thus we suggest incorporating the videos that are presented here as supplementary material (Supplementary material 1 - 14) into to the final JoVE video production to demonstrate representative results of the procedures that are described in the

	protocol.
<b>Additional Information:</b>	
<b>Question</b>	<b>Response</b>
If this article needs to be "in-press" by a certain date, please indicate the date below and explain in your cover letter.	

RE: 2D and 3D echocardiography in the axolotl (*Ambystoma mexicanum*)

---

## Cover letter

Dear JoVE editor.

Please find attached our invited submission (invited by Science Editor Indrani Mukherjee, PhD, on June 6, 2017) of a JoVE protocol on 2D and 3D echocardiography in the axolotl. The axolotl salamander is a widely applied model species in regenerative biology and this species is increasingly being applied as a model for intrinsic heart regeneration. Contrary to the zebrafish, another well-established model in heart regeneration, the axolotl can attain sizes that allows for reproducible measurements of cardiac function. Since heart regeneration is ultimately a matter of restoring function rather than only cardiac anatomy, this renders the axolotl as an important cardioregenerative model for functional regeneration and recovery.

In this submission we strive to establish the methods to perform meaningful and reproducible echocardiography on the axolotl heart to evaluate function. We provide methods to measure cardiac function in both anesthetized (demonstrating three different anesthesia regimes) and unanesthetized axolotls using 2D echocardiography. We demonstrate how to measure and minimize subjectivity and operator bias in ultrasound measurements using intra/inter-operator/observer analysis. Finally, we establish a method to acquire three-dimensional echocardiographic data on the beating axolotl heart at a high spatiotemporal resolution. Our methods have been developed and refined in the axolotl, but could find uses in other amphibians as well (e.g. *Xenopus*)

We hope that you find this contribution of value to the readers/user of JoVE and are looking forward to communicate about the manuscript.

Kind regards

Henrik Lauridsen  
Assistant Professor

**Henrik Lauridsen**

Assistant Professor

Date: 31 July 2017

Direct Tel.: +4578456106  
E-mail: henrik@clin.au.dk

Web:  
<http://au.dk/en/henrik@clin>

Sender's CVR no.: 31119103

Page 1/1

**TITLE:**

2D and 3D Echocardiography in the Axolotl (*Ambystoma Mexicanum*)

**AUTHORS & AFFILIATIONS:**

Anita Dittrich<sup>1</sup>, Mathias Møller Thygesen<sup>1</sup>, Henrik Lauridsen<sup>1</sup>

<sup>1</sup>Department of Clinical Medicine, Aarhus University, Denmark

**E-MAIL ADDRESSES:**

Anita Dittrich (adit88@gmail.com)

Mathias Møller Thygesen (maththyg@rm.dk)

Henrik Lauridsen (henrik@clin.au.dk)

**CORRESPONDING AUTHOR:**

Henrik Lauridsen, PhD (henrik@clin.au.dk)

Tel: +45 78456106

**KEYWORDS:**

Echocardiography, ultrasound, heart, cardiac ultrasonography, regeneration, axolotl, *Ambystoma mexicanum*, spatiotemporal image correlation

**SHORT ABSTRACT:**

Here we present echocardiography protocols for two-dimensional and three-dimensional image acquisition of the beating heart of the axolotl salamander (*Ambystoma mexicanum*), a model species in heart regeneration. These methods allow for longitudinal evaluation of cardiac function at a high spatiotemporal resolution.

**LONG ABSTRACT:**

Cardiac malfunction as a result of ischemic heart disease is a major challenge, and regenerative therapies to the heart are in high demand. A few model species such as zebrafish and salamanders that are capable of intrinsic heart regeneration hold promise for future regenerative therapies for human patients. To evaluate the outcome of cardioregenerative experiments it is imperative that heart function can be monitored. The axolotl salamander (*A. mexicanum*) represents a well-established model species in regenerative biology attaining sizes that allows for evaluation of cardiac function. The purpose of this protocol is to establish methods to reproducibly measure cardiac function in the axolotl using echocardiography. The application of different anesthetics (benzocaine, MS-222, and propofol) is demonstrated, and the acquisition of two-dimensional (2D) echocardiographic data in both anesthetized and unanesthetized axolotls is described. 2D echocardiography of the three-dimensional (3D) heart can suffer from imprecision and subjectivity of measurements, and to alleviate this phenomenon a solid method, namely intra/inter-operator/observer analysis, to measure and minimize this bias is demonstrated. Finally, a method to acquire 3D echocardiographic data of the beating axolotl heart at a very high spatiotemporal resolution and with pronounced blood-to-tissue contrast is described. Overall, this protocol should provide the necessary methods to evaluate cardiac function and model anatomy, and flow dynamics in the axolotl using ultrasound imaging with

applications in both regenerative biology and general physiological experiments.

## INTRODUCTION:

Ischemic heart disease is a leading cause of death worldwide<sup>1, 2</sup>. Although many survive a myocardial infarction due to rapid and fine-tuned medical intervention, ischemic incidents in humans often lead to fibrotic scarring associated with hypertrophy, electrical malfunction, and a diminished functional capacity of the heart. This lack of regenerative potential of cardiac tissue is shared among mammals and although controversial claims of mammalian cardiac regeneration have been reported, these have been limited to specific murine strains<sup>3, 4</sup> and hypoxia treated mice<sup>5</sup>. Thus, the field of cardiac regenerative medicine and biology is generally limited to non-mammalian animal models to study intrinsic heart regenerative phenomena. The zebrafish (*Danio rerio*) has in the past decade been established as the most well characterized model for intrinsic heart regeneration<sup>6-10</sup>. Due to easy laboratory maintenance, a short generation time and a wide array of molecular tools available, the zebrafish is well adapted as a model for genetic and molecular mechanisms underlying cardiac development and regeneration. However, the minute dimensions of the zebrafish heart make it less suited for functional evaluation, and complicated surgical procedures and the non-tetrapod phylogeny of the zebrafish limits the sensible extrapolation of findings in this species, thus justifying the use of other larger tetrapod models. One of the earliest models of vertebrate heart regeneration was a caudate amphibian, the Eastern newt (*Notophthalmus viridescens*)<sup>11</sup>, a species that remains a valuable model<sup>12</sup>.

In recent years another caudate amphibian, the Mexican axolotl (*A. mexicanum*) has entered the scene as a large (up to 100 g of body mass) and highly laboratory adaptable animal model for a wide array of regenerative disciplines spanning limb regeneration, spinal cord injury, and cardiac regeneration<sup>13-17</sup>. The axolotl is highly amenable to functional measurements on the heart using high frequency echocardiography and the absence of calcified structures on the ventral side of the heart allows for ultrasound imaging with a much lower level of image artifacts (acoustic shadowing and reverberation in particular) than observed in other model animals with calcified sternum and ribs.

The following protocol describes several different methods and preparations (**Figure 1, Figure 2**) to acquire reproducible echocardiographic measurements on the axolotl heart in both anesthetized (applying three different anesthetics: benzocaine, MS-222, and propofol) and unanesthetized animals in two (**Figures 3–7, Supplementary Files 1–12**) and three (**Figure 8, Figure 9, Supplementary Files 13–14**) spatial dimensions. The amphibian heart is three-chambered (two atria and a single ventricle). The atria are supplied by a large sinus venosus and the ventricle empties into the conus arteriosus outflow tract (**Figure 2**). Since most emphasis is traditionally placed on ventricular regeneration and less on the recovery of atria<sup>6-12, 14, 17</sup>, this protocol mainly focuses on measurements of ventricular function.

Amphibian echocardiography is not well-described in the literature, and the development of the 2D methods described in this paper have been driven by the need to best represent the functionality of the beating axolotl heart at a given time and experimental setting. Thus, the methods described here are applicable in heart regenerative experiments where cardiac function

can be repeatedly monitored over the course of a regeneration process. Additionally, the methods can be applied in cardiophysiological experiments on the axolotl in general or modified slightly to span other caudate or anuran amphibian models (*e.g.*, *Xenopus*). The axolotl exists in several different strains and color variations (*e.g.*, wildtype, melanoid, white, albino, transgenic white with green fluorescence protein expression), however these characteristics do not affect the compatibility of the axolotl with the described protocol. The method described here to acquire 3D echocardiographic data is a modified version of the spatiotemporal image correlation (STIC) technique developed for clinical ultrasound and the quadratic averaging method described previously in the developing chicken to enhance the signal of blood speckles in soft tissues in species containing nucleated red blood cells<sup>18, 19</sup>. This method allows for advanced modeling of cardiac contraction and computed fluid dynamics in the axolotl heart.

## **PROTOCOL:**

The procedures carried out in this protocol were in accordance with the national Danish legislation for care and use of laboratory animals and the experiments were approved by the Danish National Animal Experiments Inspectorate (protocol# 2015-15-0201-00615).

### **1. Preparations**

#### **1.1) Prepare axolotl medium.**

1.1.1) Apply high quality non-chemically treated tap water as axolotl medium. If this is unavailable, apply 40% Holtfreter's solution.

1.1.2) Prepare 40% (wt/vol) Holtfreter's solution by dissolving 15.84 g NaCl, 0.54 g CaCl<sub>2</sub>·2H<sub>2</sub>O, 1.11 g MgSO<sub>4</sub>·7H<sub>2</sub>O, and 0.288 g KCl in filtered and deionized water up to a volume of 1 L.

#### **1.2) Make immersion anesthetics.**

1.2.1) Prepare benzocaine (ethyl 4-aminobenzoate) anesthetic solution by dissolving 200 mg ethyl 4-aminobenzoate in 3 mL acetone and then dissolving this mix in 1 L tap water or 40% Holtfreter's solution.

1.2.2) Prepare MS-222 (ethyl 3-aminobenzoate methanesulfonic acid, also commonly known as tricane) anesthetic solution by dissolving 200 mg ethyl 3-aminobenzoate methanesulfonic acid directly in 1 L tap water or 40% Holtfreter's solution.

1.2.3) Prepare propofol (2,6-diisopropylphenol) anesthetic solution by dissolving 3.3 mg 2,6-diisopropylphenol in 1 L tap water or 40% Holtfreter's solution. Alternatively, dilute commercially premade solution to 3.3 mg/L.

**CAUTION:** Propofol is a powerful human anesthetic (intravenously administered) and should be handled with care, including in the diluted form.

1.3) Prepare bed and container for echocardiography.

1.3.1) Prepare lip-shaped animal bed for echocardiography by folding a 70 cm x 55 cm piece of soft cloth once and then rolling it into “burrito shape” (**Figure 1A**). Then bend over the ends until they meet and tape these together (**Figure 1B**).

1.3.2) Submerge the lip shaped structure in axolotl medium to accommodate the anesthetized axolotl during ultrasound imaging. Secure the animal to the structure and prevent floating using loose rubber bands; position these mid-mandibular and over the sacral region (**Figure 1C**).

Note: The rubber bands should not squeeze the animal as this will affect hemodynamics.

1.3.3) For 2D echocardiography on unanesthetized axolotls, prepare a hammock by carving out a 16 cm x 8 cm x 5 cm hole in a 33 cm x 27 cm x 5 cm block of polystyrene foam (*e.g.*, a lid from a medium size polystyrene foam container) (**Figure 1D**).

1.3.4) Push a 33 cm x 27 cm piece of plastic wrap through the hole and secure the edges of the wrap to the top surface of the polystyrene foam block (**Figure 1E**) to create a hammock. Add axolotl medium to 3 cm of depth in the hammock. The unanesthetized axolotl will sink to the bottom of the hammock allowing for easy ventral access through the plastic wrap (**Figure 1F**).

## 2. Anesthetize Axolotls

2.1) Immerse axolotl in desired anesthetic solution (benzocaine, MS-222, or propofol).

2.2) Inspect for first signs of sedation, reduced movements and increasing loss of righting reflex, this appears within 10 min in animals < 10 g (< 10 cm) and within 20 min in animals between 10 g and 50 g of body mass (10–22 cm).

2.3) Inspect for complete lack of body movements, gill ventilation movements, and righting reflex, and make sure the animal is non-responsive to moderate pain stimulation tested by pinching the webbing between digits.

Note: Despite the fact that general anesthesia is accomplished within 30 min in benzocaine anesthetized axolotls, cardiac function is not stabilized until 1 h. This is not the case in MS-222 or propofol anesthetized axolotls (**Figure 6A–F**).

2.4) To maintain axolotl under general anesthesia, keep the animal in anesthesia solution or wrapped in wet paper wipes wetted in anesthesia solution.

Note: Anesthesia can be maintained for 7 h without adverse effects on animal’s wellbeing given that the skin and especially the gills are kept moist.

2.5) To reawake axolotl, transfer the animal to anesthesia-free medium.

Note: The first sign of awakening is gill ventilation movements. Animal should be upright and responsive to stimulation within 1 h.

### 3. 2D Echocardiography on Anesthetized Axolotl

3.1) Place anesthetized axolotl in a supine position in the lip-shaped animal bed (steps 1.3.1–1.3.2). Secure it from floating using loose rubber bands (**Figure 1C**). Ensure that the thoracic surface is covered by 3–5 mm of medium.

Note: For a brief acquisition (< 5 min) anesthetic-free medium can be applied. For prolonged acquisition, anesthetic solution should be applied as ultrasound medium to ensure stable cardiac function throughout measurements.

3.2) Position the transducer over the midline of the animal in the thoracic region parallel to the long axis of the animal (**Figure 2A, Figure 3A-B, Supplementary File 2**). Use transillumination with a cold light source on white and albino axolotls to ensure the correct placement of the transducer (**Figure 2C and Supplementary File 1**).

3.2.1) For axolotls weighing < 20 g, use a 50 MHz transducer; for axolotls > 20 g, use a 40 MHz transducer. Ensure positioning of the cranial/anterior direction to the right for standardized image acquisition. If this is not the case rotate the transducer 180 ° or invert the image.

3.3) Make sure that in the long axis midline view, a small portion of the ventricle (positioned to the right in the thoracic cavity, **Figure 2A**) appears in the frame at ventricular diastole and a large portion of the left and right atria (positioned at the center/slightly toward the left in the thoracic cavity, **Figure 2A**) and the sinus venosus are visible both in atrial systole and diastole (**Figure 3A, B**).

3.4) Translate the transducer 1–3 mm toward the animal's right to obtain the ventricular long axis view (**Figure 2A**). The correct position is attained when the cross-sectional area of the end-systole ventricle is at its maximum (**Figure 3C–H**).

3.5) In B-mode, acquire ≥ 3 cardiac cycles with > 50 frames/s in either 'general imaging' (high spatial/low temporal resolution) or 'cardiology' (low spatial/high temporal resolution) mode.

Note: This view allows for evaluation of ventricular function. Ventricular function can be evaluated in two dimensions using the ventricular fractional area change (FACv) calculated from the end-diastolic and end-systolic cross sectional area of the ventricle (CSAv) using the equation:

$$FACv = \frac{CSAv(diastole) - CSAv(systole)}{CSAv(diastole)}$$

(1)

The axolotl's ventricle assumes the shape of a sphere and a geometry based stroke volume



[SV(geo)] can be calculated using the equation:

$$SV(geo) = \frac{4}{3}\pi \times \left( \left( \frac{CSAv(diastole)}{\pi} \right)^{\frac{3}{2}} - \left( \frac{CSAv(systole)}{\pi} \right)^{\frac{3}{2}} \right) \quad (2)$$

3.6) Translate the transducer along the long axis of the animal until the center of the ventricle is in the middle of the screen. Rotate the transducer 90 ° clockwise to obtain the mid-ventricular short axis view (**Figure 5A and B, Supplementary File 10**). Evaluate the circular shape of the ventricle by translating the transducer along the long axis of the heart.

3.7) Return the transducer to the long axis plane and translate it back toward the midline or slightly to the left of the midline to obtain the atrial long axis two chamber view (**Figure 2A**). Make sure that the correct position is attained by confirming that the cross-sectional areas of the end-systole atria are at their maxima and the two atria combined assume the outline of the number '8' tilted ~ 45 ° toward the left (**Figure 4A and B, Supplementary File 6**).

3.8) In B-mode acquire ≥ 3 cardiac cycles with > 50 frames/s in either 'general imaging' or 'cardiology' mode.

Note: The axolotl's atria are irregular in shape and 3D function cannot be directly inferred from 2D data, thus their function must be evaluated as an index measure such as atrial fractional area change (FACa) based on the combined cross sectional area (CSAa) of both atrial chambers in systole and diastole:

$$FACa = \frac{CSAa(diastole) - CSAa(systole)}{CSAa(diastole)} \quad (3)$$

3.9) Translate the transducer toward the right until the outflow tract (conus arteriosus) appears (close to the ventricular long axis view) (**Figure 2A**).

Note: After leaving the ventricle in an anterior direction, the outflow tract makes a sharp bend and runs at a small angle toward the ventral surface before again assuming an anterior direction and splitting up into gill branches and systemic vessels.

3.9.1) Make sure that the correct outflow tract view is attained by confirming that the diameter of the outflow is at its maximum at ventricular end-systole and two of the three semilunar valves at the entrance of the outflow are visible at mid-ejection (**Figure 4E, Supplementary File 8**).

Note: The ventral directionality toward the transducer of the intermediate portion of the outflow tract allows for velocity and flow measurements using Doppler imaging.

3.10) Apply Color Doppler-mode to map blood flow velocities in the outflow tract during cardiac ejection (**Figure 4F and Supplementary File 9**). Likewise apply Color Doppler and Power Doppler imaging to visualize blood flow in the ventricular and atrial views (**Figure 3E–H, Supplementary Files 4-5 and Figure 4C-D, and Supplementary File 7**).

3.11) Apply Pulse Wave (PW) Doppler-mode at the position of maximum blood velocity in the portion of the outflow tract running toward the transducer.

3.11.1) Use 'beam angle' and 'angular correction' up to 45 ° to adjust for the outflow not being completely perpendicular to the face of the transducer (**Figure 4G**). Make sure that the PW Doppler position is not overlapped by the spiral valve of the outflow during any phase of the cardiac cycle (**Figure 4E**).

3.12) In PW Doppler-mode acquire velocity/time data over  $\geq 3$  cardiac cycles.

3.13) Return to B-mode and acquire  $\geq 3$  cardiac cycles at the exact same plane as PWV was acquired.

3.14) Measure the velocity time integral (VTI) of the blood flow in the outflow tract as the area under the velocity/time curve for one full cardiac cycle (**Figure 4G, g1**).

Note: From the VTI and the diameter (d) of the outflow tract at end-systole obtained from the B-mode acquisition, a PW Doppler based stroke volume [SV(pw)] can be calculated using the equation:

$$SV(pw) = \left(\frac{d}{2}\right)^2 \times \pi \times VTI \quad (4)$$

Heart rate (HR) is measured from the velocity/time curve by measuring the duration of an entire cardiac cycle. Cardiac output [CO(pw)] is calculated using the equation:

$$CO(pw) = SV(pw) \times HR \quad (5)$$

3.15) Obtain the oblique paragill view, a view that offers an alternative for the measurement of the blood flow velocity in the outflow tract, by rotating the axolotl 90 ° in the lip shaped bed in such a way that the right part of the animal is facing upward (**Figure 2B**). Angle and rotate the transducer and position it parallel and just posterior to the protruding gills (**Figure 2B**). Make sure that the correct position is attained by confirming that the outflow tract is running downward at  $\sim 45^\circ$  and that the atria appear under the outflow tract during ejection (**Figure 5C, Supplementary File 11**).

3.16) Apply PW Doppler-mode at the position of maximum blood velocity in the portion of the outflow tract running away from the transducer (**Figure 5D, Supplementary File 12**). Use 'beam angle' and 'angular correction' up to 45 ° to adjust for the outflow not being completely

perpendicular to the face of the transducer (**Figure 5E**).

3.17) In the PW Doppler-mode acquire blood velocity over  $\geq 3$  cardiac cycles.

3.18) Return to B-mode and acquire  $\geq 3$  cardiac cycles at the exact same plane as PWV was acquired.

Note: SV(pw) and CO(pw) are calculated for the oblique parasternal view using **Equation 4** and **Equation 5** as described above for the long axis view.

#### **4. 2D Echocardiography on Unanesthetized Axolotl**

4.1) Place the unanesthetized axolotl in a prone position in the hammock (step 1.3.3).

4.2) Leave the animal undisturbed for 30–60 min to recover from handling stress.

4.3) Position the ultrasound transducer with the transducer head facing upward toward the axolotl in the hammock.

4.4) Apply ultrasound-gel on the transducer.

4.5) Gently, and without disturbing the animal, position the transducer over the midline of the animal in the thoracic region parallel to the long axis of the animal.

Note: This is the same, but inverted, position as for the anesthetized axolotl (step 3.2).

4.6) Obtain B-mode, Color Doppler mode, PW mode data in the long axis and short axis view as described in steps 3.2–3.14.

Note: An oblique parasternal view is unobtainable in the unanesthetized axolotl. The echocardiographic data in unanesthetized axolotls should be acquired between gill ventilation movements (a 10–20 s period for a resting animal). If the axolotl moves during acquisition, measurements must be repeated.

#### **5. Evaluate 2D Echocardiography Data and Minimize Subjectivity**

5.1) Avoid operator/observer bias in 2D ultrasound imaging and 3D evaluation of cardiac function based on 2D data caused by subjectivity in both the data acquisition and the data analysis phase by performing intra/inter-operator/observer analysis<sup>20</sup>.

Note: In the startup of studies and when training new personnel this subjectivity must be quantified and minimized using intra/inter-operator/observer analysis.

5.2) Initiate the intra/inter-operator/observer analysis in a two person setup with

operator/observer 1 (less experienced) being tested against operator/observer 2 (more experienced) by performing  $\geq 6$  consensus measurements together, including both bench work at the ultrasound system (operation) and subsequent analysis of relevant parameters (observation).

5.3) Reach consensus between operators and observers and operate (operator/observer 1) the ultrasound system to acquire relevant data on  $\geq 6$  animals (operation 1.1).

5.4) Directly after, operate (operator/observer 2) the ultrasound system to acquire relevant data on the same animals (operation 2.1).

5.5) Let animals recover for 3 days. Thereafter, repeat (operator/observer 1) the procedure (operation 1.2).

5.6) Analyze (operator/observer 1) all measured data (operation 1.1/observation 1.1; operation 2.1/observation 1.1; operation 1.2/observation 1.1) and after 24 h repeat the analysis of operator/observer 2's data (operation 2.1/observation 1.2).

5.7) Analyze (operator/observer 2) the data acquired by her/himself (operation 2.1/observation 2.1). Note that the values obtained by this analysis are considered closest to the true values.

5.8) Evaluate variation, tendencies, and bias in comparisons between all acquired parameters using Bland-Atman plotting, QQ plotting, *t*-test (equal mean), and *F*-test (equal variance) (**Figure 6G**).

5.8.1) Note that the operation 1.1/observation 1.1 versus operation 2.1/observation 1.1 comparison demonstrates the inter-operator variation.

5.8.2) Note that the operation 2.1/observation 1.1 versus operation 2.1/observation 2.1 comparison demonstrates the inter-observer variation.

5.8.3) Note that the operation 1.1/observation 1.1 versus operation 1.2/observation 1.1 comparison demonstrates the intra-operator variation.

5.8.4) Note that the operation 2.1/observation 1.1 versus operation 2.1/observation 1.2 comparison demonstrates the intra-observer variation.

5.9) Make sure that mean and variation of the different measurements are non-significantly different for the four comparisons; the difference between measured values should fall within  $\pm 1.96$  standard deviations, and there should appear no tendencies toward less precision of neither small nor large values.

## **6. 3D Echocardiography on Anesthetized Axolotl**

## 6.1) 3D acquisition

6.1.1) Place the anesthetized axolotl in a supine position in the lip-shaped animal bed (step 1.3.1). Secure it from floating using loose rubber bands (**Figure 1C**) and make sure that the thoracic surface is covered by 3–5 mm of medium. 3D acquisition is a lengthy procedure, therefore apply anesthetic solution as ultrasound medium to ensure stable cardiac function throughout measurements.

6.1.2) Position the transducer over the midline of the animal in the thoracic region either parallel to the long axis of the animal (for a sagittal 3D recording) or orthogonal to the long axis (transversal 3D recording).

6.1.3) Translate the transducer in the in-plane dimension ( $x$  and  $y$ ) and the out-of-plane dimension ( $z$  or slice) to ensure that the entire cardiac region will be covered in the subsequent 3D capture.

6.1.4) Adjust the frame rate and spatial resolution as desired by selecting either ‘general imaging’ (high spatial/low temporal resolution) or ‘cardiology’ (low spatial/high temporal resolution) mode. For  $0.33 \text{ Hz} < \text{HR} < 1 \text{ Hz}$  use a temporal resolution of 50 frames/s obtained at high spatial resolution (‘general imaging’) that allows for the cardiac cycle to be reconstructed into 50–150 distinct phases.

6.1.5) Adjust ‘2D gain’ to a level where anatomical structures are barely recognizable in the raw B-mode image ( $\sim 5 \text{ dB}$ ) to increase signal-to-noise-ratio in the final reconstructions.

6.1.6) For each slice ( $z$  step), record  $\geq 1,000$  frames.

6.1.7) Translate transducer one  $z$  step at a time, *e.g.*,  $20 \mu\text{m}$  or  $50 \mu\text{m}$ , and repeat recording until the entire cardiac region is covered.

## 6.2) 3D reconstruction (**Supplementary Files 13 and 14**).

6.2.1) Export acquisitions into Digital Imaging and Communications in Medicine DICOM (little endian).

Note: Each slice containing a set number of frames will compose a single file.

6.2.2) Determine the number of frames in a full cardiac cycle. As HR can vary over time, determine this for both the first and the final slice. Set the highest number of frames per cycle as the initial upper estimation of phase resolution that can later be reduced (step 6.2.8).

6.2.3) Determine crop boundaries and excise irrelevant space surrounding the B-mode window.

Note: These boundaries should be constant throughout slices.

6.2.4) Convert the RGB Color image into 32-bit.

6.2.5) Calculate the correlation value (C) for each frame in the stack and the number of frames included in the first cardiac cycle using the formula:

$$C = \frac{1}{I \times J} \sum_{j=1}^J \sum_{i=1}^I \frac{[SI_1(i,j) - AVG_1][SI_2(i,j) - AVG_2]}{SD_1 SD_2} \quad (6)$$

Note: Here  $SI_1(i, j)$  is the signal intensity of the pixel at coordinate  $(i, j)$  in the first image and  $SI_2(i, j)$  is the same in the second image,  $AVG_1$ ,  $AVG_2$  and  $SD_1$ ,  $SD_2$  are the mean intensity and standard deviation, respectively, of the first and second image in the comparison, and  $I$  and  $J$  are the numbers of columns and rows in the image. The resulting array of correlation values will have the size of the product of the number of frames per cardiac cycle and the total number of frames per slice (*e.g.*,  $75 \times 1,000 = 75,000$  in **Figure 8**) (see exemplary script in **Supplementary File 16**). The correlation value cannot be calculated if one or both of the images in the comparison have a standard deviation of pixel values of zero, however this is highly unlikely in ultrasonographic images.

6.2.6) Detect local maxima in the array of correlation values (**Figure 8A**, see exemplary script in **Supplementary File 17** to automatically detect local maxima).

6.2.7) Calculate quadratic average  $Q(AVG)$  of frames with peak correlation values (*i.e.*, matching cardiac phases) using the formula:

$$Q(AVG)_{ij} = \left( \frac{1}{N} \sum_{n=1}^N [SI_n(i, j) - \overline{SI_n}]^2 \right)^{\frac{1}{2}} \quad (7)$$

where  $N$  is the total number of frames with matching cardiac phases,  $SI_n(i, j)$  is the intensity of the pixel at coordinate  $(i, j)$  of the  $n^{\text{th}}$  image and  $\overline{SI_n}$  is the temporal arithmetic mean of  $SI_{ij}$  of the  $n^{\text{th}}$  image (see exemplary script in **Supplementary File 18**).

6.2.8) Repeat step 6.2.3–6.2.7 for all slices.

6.2.9) Select a slice (reference slice) with easily recognizable anatomical structures (*e.g.*, mid-ventricular) and check if the reconstructed ensemble averaged one cardiac cycle corresponds to exactly one cycle (*i.e.*, if there are additional phases resulting in more than one cardiac cycle). Delete additional phases to yield exactly one cardiac cycle (*e.g.*, going from an overestimated 75 phases/cycle (in reality, 1.07 cycle) in **Figure 8** to exactly one cycle containing 70 phases in **Figure 8**).

6.2.10) On the neighboring slice (test slice), sort the ensemble averaged one cardiac cycle *t*-stack into matching cardiac phases with the reference slice using the correlation value formula (**Equation 6**) (see exemplary scripts in **Supplementary File 19** and **Supplementary File 20**).

Note: Although two non-identical slices will not appear completely similar at any point during the cardiac cycle, adjacent slices with a sufficiently small step size (*e.g.*, 20  $\mu\text{m}$  or 50  $\mu\text{m}$ ) will have pronounced similarities resulting in correlation value maxima that can be translated into matching phases.

6.2.11) Repeat step 6.2.9–6.2.10 for all slices.

6.2.12) Collapse the entire 3D reconstruction into a single 3D Tagged Image File format (TIF) containing *z* slices and *t* frames or into a stack of DICOM files.

Note: Data can be binned in each dimension to reduce size, increase signal-to-noise ratio and generate isotropic data (in-plane resolution is usually several folds higher than out-of-plane resolution).

#### **REPRESENTATIVE RESULTS:**

Intrapericardial space in the axolotl is dependent on the size of the animal. Smaller animals (2–20 g, 7–15 cm) will have an excess of pericardial fluid (appearing dark in echocardiography) surrounding the cardiac chambers whereas in larger sexually mature animals (> 20 g, > 15 cm) the chambers will occupy most of the intrapericardial space. To provide the best overview for representative results of echocardiographic views of the axolotl heart, a smaller animal (10 g, 10 cm) was applied for **Figures 3–5**, and **Figure 9**.

The long axis view generally provides a good overview of cardiac anatomy in the axolotl. Entering at the midline plane with the sinus venosus, atria, and part of the ventricle in plane (**Figure 3A, B, Supplementary File 2**), either the ventricular plane (**Figure 3C–H**) or the atrial plane (**Figure 4A–D**) can be reached by translating the transducer to the right or left of the animal, respectively. The ventricle will appear spherical and highly trabeculated (**Figure 3C, Supplementary Files 3–5**), whereas the atria have a more irregular shape and almost no trabeculation (**Figure 4A, Supplementary File 6, Supplementary File 7**). The short axis view (**Figure 5A, B, Supplementary File 10**) provides a less easily interpretable overview of the cardiac anatomy of the axolotl heart, however it contributes to the evaluation of correct cardiac contraction (*e.g.*, infarcted or non-contracting zones of the circular ventricle are clearly visualized in this view plane). In the long axis view plane, the center of the outflow tract is positioned closely to the center of the ventricle (**Figure 2A**, and compare **Figure 3C** with **Figure 4E** and **Supplementary File 3** with **Supplementary File 8**). Since the soft tissue of the outflow tract will be moving upon blood ejection, the high intensity blood signal during a cardiac cycle measured by pulse wave Doppler in both the long axis and the oblique paragill plane will be adjoined by low intensity noise from the movements of the surrounding soft tissue (gray area surrounding white area in the velocity/time curve in **Figure 4G** and **Figure 5E**). Generally, the contrast between blood signal and soft tissue noise

should be large enough to segment out only the blood signal when measuring the velocity time integral (**Figure 4G** (g1 magnification) and **Figure 5E** (e1 magnification)).

For qualitative evaluation of blood flow patterns, color Doppler and power Doppler imaging provide visualizations of flow patterns in different cardiac chambers (ventricle: **Figure 3E–H**, **Supplementary File 4**, **Supplementary File 5**; atria: **Figure 4C, D**, **Supplementary File 7**; outflow tract: **Figure 4F**, **Figure 5D**, **Supplementary File 9**, **Supplementary File 12**).

Axolotls used for laboratory experimentation vary in size from the early post larval stage of 2–4 g to full maturity at 10–30 g and larger animals weighing > 100 g. Likewise, cardiac function and some absolute values of functional parameters described here depend on the size of the animals. Generally, fractional area change is constant in different size groups with values ranging at 40–50% (skewed toward lower values for larger animals). Stroke volume is highly dependent on the size of the animal, *i.e.*, the size of the heart, ranging from *e.g.*, 20–30  $\mu\text{L}$  in 5 g axolotls, 50–70  $\mu\text{L}$  in 10 g axolotls, and 250–300  $\mu\text{L}$  in 50 g axolotls. Heart rate and to some degree stroke volume are highly dependent on the applied anesthetic and the level of anesthesia (**Figure 6A–F**, **Figure 7**).

Traditional intra/inter-operator/observer analysis involves graphical representations (Q-Q Plots and Bland-Altman plots) and testing for equal mean (*t*-test) and variance (*F*-test) to evaluate normal distribution of data and to compare accuracy and precision between two persons (**Figure 6G**).

3D echocardiography adds an additional dimension (*z* or depth) to the more traditional 2D acquisition. This allows for multi-planar visualization of data (**Figure 9A**), reslicing (**Figure 9B**), surface and volume reconstructions (**Figure 9C**, **Supplementary File 13**, and **Supplementary File 14**), and segmentation and generation of 3D models (**Figure 9C**, **Supplementary File 15**).

#### FIGURE LEGENDS:

**Figure 1. Preparation of bed and container for echocardiography of anesthetized and unanesthetized axolotl.** (A) A soft piece of cloth is folded once and rolled into “burrito” shape. (B) The ends are bent back and taped to form a lip shaped bed for the axolotl during underwater scanning. (C) For 2D and 3D echocardiography of an anesthetized axolotl, the animal is gently placed in a supine position in the crevice of the lip shaped bed and fixed with rubber bands over the mid-mandibular and sacral region. (D, E) A hammock is prepared by carving out a square hole in a piece of polystyrene foam and taping plastic wrap to the upper surface. (F) For 2D echocardiography of an unanesthetized axolotl, the animal is placed in a natural prone position in the hammock and approached with a gel covered transducer tip from underneath.

**Figure 2. Transducer placement.** (A, B) Model of the arterial network in the axolotl with the approximate position of the transducer for long axis and short axis view (A) and oblique paragill view (B). (C) Transillumination with a powerful cold light source can aid in finding the exact location of the cardiac chambers before applying the transducer (see **Supplementary File 1**).



Anatomical abbreviations: A, atria; OFT, outflow tract; SinV, sinus venosus; V, ventricle.

**Figure 3. Representative long axis echocardiographic views of the ventricle.** (A, B) Typical long axis midline view in B-mode (yellow line in **Figure 2A**) in the ventricular end-diastolic (A) and end-systolic (B) phases (see **Supplementary File 2** for video representation). (C, D) Long axis view of the ventricle in B-mode (black line in **Figure 2A**) in the ventricular end-diastolic (C) and end-systolic (D) phases (see **Supplementary File 3** for video representation). (E–H) Similar view plane as in (A) and (B) in color Doppler (CD) and power Doppler (PD) mode demonstrating blood flow (see **Supplementary File 4** and **Supplementary File 5** for video representation of CD- and PD-mode, respectively). Red colors in CD-mode images indicate blood flowing toward the transducer and blue colors indicate the opposite. Cardiac chambers and blood flow have been highlighted with dotted lines. Inserted cartoons in (A) and (C) show placement of transducer and translation relative to the long axis midline view. Anatomical abbreviations: A, atria; DC(L), left duct of Cuvier; OFT, outflow tract; SinV, sinus venosus; V, ventricle.

**Figure 4. Representative long axis echocardiographic views of the atria and outflow tract.** (A, B) Long axis view of the atria in B-mode (green line in **Figure 2A**) in the atrial end-diastolic (A) and end-systolic (B) phases (see **Supplementary File 6** for video representation). (C, D) Similar view plane as in (A) and (B) in color Doppler (CD) mode demonstrating blood flow (see **Supplementary File 7** for video representation). (E) Long axis view of the outflow tract in B-mode (blue line in **Figure 2A**) in the mid-ejection phase (see **Supplementary File 8** for video representation). (F) Similar view plane as in (E) in CD-mode demonstrating blood flow (see **Supplementary File 9** for video representation). (G) Similar view plane as in (E) and (F) in pulse wave Doppler (PW) mode allowing for heart rate detection and velocity time integral (VTI) measurement for stroke volume calculation. Red colors in CD-mode images indicate blood flowing toward the transducer and blue colors indicate the opposite. Cardiac chambers and blood flow have been highlighted with dotted lines. Yellow and red arrow heads indicate semilunar valves at the root of the outflow tract and the spiral valve in the outflow tract, respectively. Inserted cartoons in (A) and (E) show placement of transducer and translation relative to the long axis midline view. Anatomical abbreviations: A(R), right atrium; A(L), left atrium; OFT, outflow tract; SinV, sinus venosus; V, ventricle; VC, vena cava.

**Figure 5. Representative short axis and oblique parasternal echocardiographic views of the ventricle and outflow tract.** (A, B) Short axis view of the ventricle in B-mode (grey line in **Figure 2A**) in the ventricular end-diastolic (A) and end-systolic (B) phases (see **Supplementary File 10** for video representation). (C) Oblique parasternal view of the outflow tract in B-mode (purple line in **Figure 2B**) in the mid-ejection phase (see **Supplementary File 11** for video representation). (D) Similar view plane as in (C) in CD-mode demonstrating blood flow (see **Supplementary File 12** for video representation). (E) Similar view plane as in (C) and (D) in pulse wave Doppler (PW) mode allowing for heart rate detection and velocity time integral (VTI) measurement for stroke volume calculation. Red colors in CD-mode images indicate blood flowing toward the transducer and blue colors indicate the opposite. Cardiac chambers and blood flow have been highlighted with dotted lines. Inserted cartoons in (A) and (C) show placement of transducer and translation relative to the long axis midline view. Anatomical abbreviations: A, atria; OFT, outflow tract; SinV, sinus

607 venosus; V, ventricle.

608  
609 **Figure 6. Representative results of heart rate and stroke volume measurements, the effect of**  
610 **anesthesia, and representative intra/inter-operator/observer analysis. (A–C)** Heart rate (HR)  
611 relative to unanesthetized baseline plotted over time (0 h is at full anesthesia) for six axolotls  
612 anesthetized in benzocaine (A), MS-222 (B), and propofol (C). (D–F) Stroke volume (SV) relative  
613 to unanesthetized baseline plotted over time (0 h is at full anesthesia) for six axolotls  
614 anesthetized in benzocaine (D), MS-222 (E), and propofol (F). (G) Intra/inter-operator/observer  
615 analysis of stroke volume. Bland-Altman plots [difference (Dif) between operators  
616 (Op)/observers (Obs) plotted against average (Avg)] should reveal no systematic bias in the  
617 normally distributed measurements (Q-Q Plots) obtained by different operators and observers.  
618 Testing for equal mean (*t*-test) and equal variance (*F*-test) should reveal no significant differences  
619 between operators/observers (table in lower right). A–F was modified from material available  
620 under the Creative Commons Attribution License (Figure 1 of Thygesen *et al.*<sup>21</sup>).

621  
622 **Figure 7. Comparison of stroke volume estimated by the geometric and the pulse wave Doppler**  
623 **method.** Comparison of stroke volume (SV) estimated by either two-dimensional B-mode  
624 geometric (geo) measurements or pulse wave Doppler measurements on the velocity of blood  
625 exiting the outflow tract. SV(geo) and SV(pw) is recorded in the same six animals with seconds in  
626 between the two measurement types and using three different anesthetics, benzocaine (blue  
627 tilted squares), MS-222 (red squares), and propofol (green triangles) with one week of recovery  
628 between applying the different anesthetics.

629  
630 **Figure 8. Representative spatiotemporal image correlation for 3D echocardiography. (A)** Curve  
631 representation of yielded correlation values of a correlation operation in a 1,000 frame cine  
632 dataset with 75 frames per cardiac cycle. Two frames with only small differences, indicating  
633 matching cardiac phases, will yield a high correlation value. Subsequently a local maxima  
634 searching algorithm can be applied on the data to detect all matching frames. (B) Graphical  
635 representation of the same data as in (A). When correlation values are obtained by comparing  
636 the first cardiac cycle with the entire cine stack, diagonal lines of maximum correlation indicate  
637 matching cardiac phases.

638  
639 **Figure 9. Representative 3D echocardiography. (A)** Multi-planar view of 3D reconstructed axolotl  
640 heart. The spatiotemporal image correlation procedure allows for the reconstruction of a full  
641 cardiac cycle with several distinct phases (here 70 phases) in three spatial dimensions that can  
642 then be sliced as ones for desired investigation of spatiotemporal phenomena in the beating  
643 heart. (B) Three transversal slices of the reconstructed 115 slices 3D data. The quadratic  
644 averaging procedure enhances the blood-to-tissue contrast and lowers the signal-to-noise ratio  
645 allowing for a better appreciation of the trabeculated nature of the axolotl ventricle and a clear  
646 visualization of the interatrial septum and the valves in the outflow tract. (C) Surface and volume  
647 representations of the beating heart at three phases along a color coded segmented model (see  
648 **Supplementary File 13** and **Supplementary File 14** for video representations of the surface and  
649 volume rendered beating heart, and **Supplementary File 15** for a three-phase segmented  
650 interactive 3D model). Anatomical abbreviations: A, atria; Cau, caudal; Cra, cranial; Dex, dexter

(to the animal right); Dor, dorsal; OFT, outflow tract; Sin, sinister (to the animals left); SinV, sinus venosus; V, ventricle; Ven, ventral.

**Supplementary File 1. Transillumination to locate cardiac chambers in the axolotl. See Figure 2C.**

**Supplementary File 2. Long axis, midline view, B-mode. See Figure 3A, B.**

**Supplementary File 3. Long axis, ventricular view, B-mode. See Figure 3C, D.**

**Supplementary File 4. Long axis, ventricular view, Color Doppler mode. See Figure 3E, F.**

**Supplementary File 5. Long axis, ventricular view, Power Doppler mode. See Figure 3G, H.**

**Supplementary File 6. Long axis, atrial view, B-mode. See Figure 4A, B.**

**Supplementary File 7. Long axis, atrial view, Color Doppler mode. See Figure 4C, D.**

**Supplementary File 8. Long axis, outflow tract view, B-mode. See Figure 4E.**

**Supplementary File 9. Long axis, outflow tract view, Color Doppler mode. See Figure 4F.**

**Supplementary File 10. Short axis, ventricular view, B-mode. See Figure 5A, B.**

**Supplementary File 11. Oblique paragill, outflow tract view, B-mode. See Figure 5C.**

**Supplementary File 12. Oblique paragill, outflow tract view, Color Doppler mode. See Figure 5D.**

**Supplementary File 13. Three-dimensional surface rendering of beating heart in 70 phases (19.6 ms temporal resolution). See Figure 9C.**

**Supplementary File 14. Three-dimensional volume rendering of beating heart in 70 phases (19.6 ms temporal resolution). See Figure 9C.**

**Supplementary File 15. Three-dimensional interactive model of beating heart in 3 phases: Ventricular end-systole, ventricular mid-ejection, and ventricular end-systole. See Figure 7C.**  
The interactive PDF file should be viewed in Adobe Acrobat Reader 9 or higher. To activate the 3D feature, click the model. Using the cursor, it is now possible to rotate, zoom, pan the model, and in the model tree all segments of the model can be turned on/off or made transparent. The model tree is a hierarchy containing several sub layers that can be opened (+).

**Supplementary File 16. Representative annotated script for calculating the correlation value of a 1,000 frames acquisition with an upper estimation of 75 frames/cardiac cycle. The script is**

written in IJ1 macro language and can be implemented as a batch macro in ImageJ to calculate correlation values (75,000 per acquisition) across an entire z-stack of 3D data.

**Supplementary File 17. Representative script for automatic peak detection in a series of correlation values from a 1,000 frames acquisition with an upper estimation of 75 frames/cardiac cycle.** The series of correlation values (Column B, marked in yellow) can be replaced and after activation of the macro (Ctrl + r) the list of commands to select matching cardiac phases and perform quadratic averaging will be displayed (Column Q, marked in green).

**Supplementary File 18. Representative annotated script to select matching cardiac phases and perform quadratic averaging of a 1,000 frames acquisition with an upper estimation of 75 frames/cardiac cycle (Column Q in Supplementary File 17).** The script is written in IJ1 macro language and can be implemented as a macro in ImageJ to create an ensemble averaged one cycle (75 phases) 2D slice.

**Supplementary File 19. Representative annotated script for calculating the correlation value between a 70 frames reference slice and an adjacent 75 frames test slice.** The script is written in IJ1 macro language and can be implemented as a macro in ImageJ to calculate correlation values (5,250).

**Supplementary File 20. Representative Excel script for automatic peak detection in a series of correlation values from a comparison between a 70 frames reference slice and an adjacent 75 frames test slice.** The series of correlation values (Column C, marked in yellow) can be replaced and after activation of the macro (Ctrl + t) the list of slices to be selected as a substack in the test slice will be displayed (Column L, Row 2, marked in green). The test slice substack will have spatially matching frames to the reference slice.

## **DISCUSSION:**

Echocardiography in the axolotl and other non-mammalian species yields fundamentally different data than mammalian echocardiography because of the nucleated nature of red blood cells in all vertebrates except adult mammals. This results in a pronounced blood signal and less blood-to-tissue contrast in axolotl echocardiographic images compared to *e.g.*, mouse or human echocardiography. This can make image segmentation on unprocessed single frame ultrasound images more difficult as it can be hard to distinguish blood from tissue. However, this phenomenon can be advantageous when used to create blood signal enhanced images by applying the quadratic averaging procedure described previously<sup>18</sup> and modified for axolotl echocardiography in Protocol Section 6. Since blood speckles are much more dynamic than those found in soft tissue, quadratic averaging will generate pronounced contrast between these two compartments which facilitates image segmentation in two and three dimensions.

This protocol describes three different anesthetics for the axolotl that have been thoroughly tested previously<sup>21</sup>. Both benzocaine and MS-222 stimulate an increase in heart rate, which can be desirable when testing cardiac function under stress conditions. Propofol induces less stress to the heart during anesthesia and may be used as a substitution for unanesthetized

echocardiography in situations where acquisition time exceeds the limits of sedentary behavior in unanesthetized axolotls.

2D echocardiography describing the 3D heart is affected by subjectivity. Therefore, it is imperative to conduct an intra/inter-operator/observer analysis before conducting an actual experiment as described in Protocol Section 5. Likewise, echocardiographic measurements should be viewed more as index values that can be applied to investigate potential differences in cardiac function under different circumstances rather than absolute values. The stroke volume determined by the geometric equation (**Equation 2**) rarely yields the same absolute value as the pulse wave Doppler equation (**Equation 4; Figure 7**), and it should be decided which measure to adhere to throughout a series of experiments. The SV(geo) can be obtained more rapidly than the SV(pw), however the spherical assumption of the ventricular shape only applies to healthy uniformly contracting hearts, and in disease and regeneration models, SV(pw) should be considered for a better reflection of the true stroke volume.

The correlation and quadratic averaging procedure of Protocol Section 6 can be implemented in several different imaging and mathematical packages. Since programming skills and access to software packages vary greatly within life science researchers, we have strived toward providing representative scripts for the methods in software packages that most researchers are familiar with (*e.g.*, Excel) that are easily approached and freely available (ImageJ: <https://imagej.nih.gov/ij/index.html>). **Supplementary Files 16–20** provide annotated exemplary scripts written in IJ1 macro language and as .xslm macros that should be comprehensible even with minimum experience in coding.

Intrinsic heart regeneration is a phenomenon exclusively found in the hearts of small species (relative to human), and thus measurements and imaging of baseline cardiac function and functional progress during regeneration is challenged by the size of the heart and the spatial resolution of the imaging modality applied. High frequency ultrasound imaging provides a desirable trade-off between a high in-plane spatial resolution ( $\sim 30 \times 30 \mu\text{m}^2$  at 50 MHz) that is comparable to *in vivo*  $\mu\text{CT}$  imaging and much higher than *in vivo*  $\mu\text{MRI}$ , which has a depth of penetration ( $\sim 1 \text{ cm}$  at 50 MHz) several fold larger than confocal microscopy, and a very high temporal resolution (50–300 frames/s at 50 MHz, 1 cm depth). Coupled with manual or automated z dimensional movement of the transducer, ultrasound enables unmatched reconstruction of cardiac function and anatomical modeling in four dimensions. Additionally, the non-invasive nature of the technique allows for longitudinal experimentation. To our knowledge there are currently no matrix array transducers available for high frequency micro ultrasound imaging. The development of this technology would greatly aid the acquisitions of 3D data of small hearts such as that of the axolotl in a faster procedure than mechanically moving the transducer.

#### **ACKNOWLEDGMENTS:**

We would like to acknowledge Kasper Hansen, Institute for Bioscience, Aarhus University for providing access to and assistance with the electronic micromanipulator for 3D echocardiographic acquisition.

**DISCLOSURES:**

The authors have nothing to disclose.

**REFERENCES:**

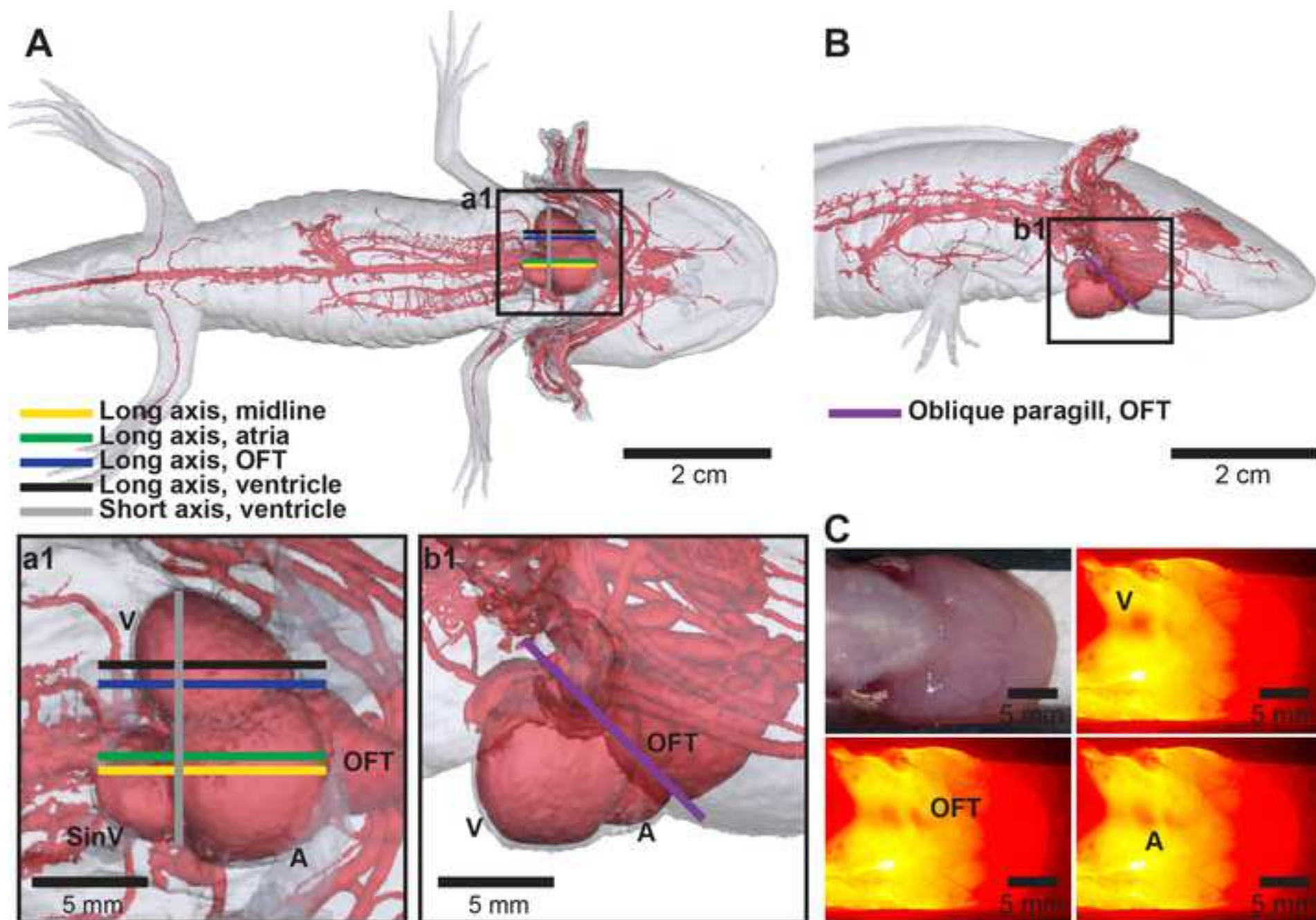
1. Forouzanfar, M.H., et al. Assessing the Global Burden of Ischemic Heart Disease. *Glob. Heart* **7**, 331–342 (2012).
2. Go, A.S., et al. Heart Disease and Stroke Statistics--2014 Update: A Report From the American Heart Association. *Circulation* **129**, e28–e292 (2014).
3. Leferovich, J.M., et al. Heart regeneration in adult MRL mice. *Proc. Natl. Acad. Sci. USA* **98**, 9830–9835 (2001).
4. Leferovich, J.M., Heber-Katz, E. The scarless heart. *Semin. Cell Dev. Biol.* **13**, 327–333 (2002).
5. Nakada, Y., et al. Hypoxia induces heart regeneration in adult mice. *Nature* **541**, 222–227 (2017).
6. Poss, K.D., Wilson, L.G., Keating, M.T. Heart regeneration in zebrafish. *Science* **298**, 2188–2190 (2002).
7. Chablais, F., Veit, J., Rainer, G., Jazwinska, A. The zebrafish heart regenerates after cryoinjury induced myocardial infarction. *BMC Dev. Biol.* **11**, 21 (2011).
8. Gemberling, M., Bailey, T.J., Hyde, D.R., Poss, K.D. The zebrafish as a model for complex tissue regeneration. *Trends. Genet.* **29**, 611–620 (2013).
9. Gonzalez-Rosa, J.M., Martin, V., Peralta, M., Torres, M., Mercader, N. Extensive scar formation and regression during heart regeneration after cryoinjury in zebrafish. *Development* **138**, 1663–1674 (2011).
10. Schnabel, K., Wu, C.C., Kurth, T., Weidinger, G. Regeneration of cryoinjury induced necrotic heart lesions in zebrafish is associated with epicardial activation and cardiomyocyte proliferation. *PLoS One* **6**(4): e18503 (2011).
11. Oberpriller, J.O., Oberpriller, J.C. Response of the adult newt ventricle to injury. *J. Exp. Zool.* **187**, 249–260 (1974).
12. Witman, N., Murtuza, B., Davis, B., Arner, A., Morrison, J.I. Recapitulation of developmental cardiogenesis governs the morphological and functional regeneration of adult newt hearts following injury. *Dev. Biol.* **354**, 67–76 (2011).

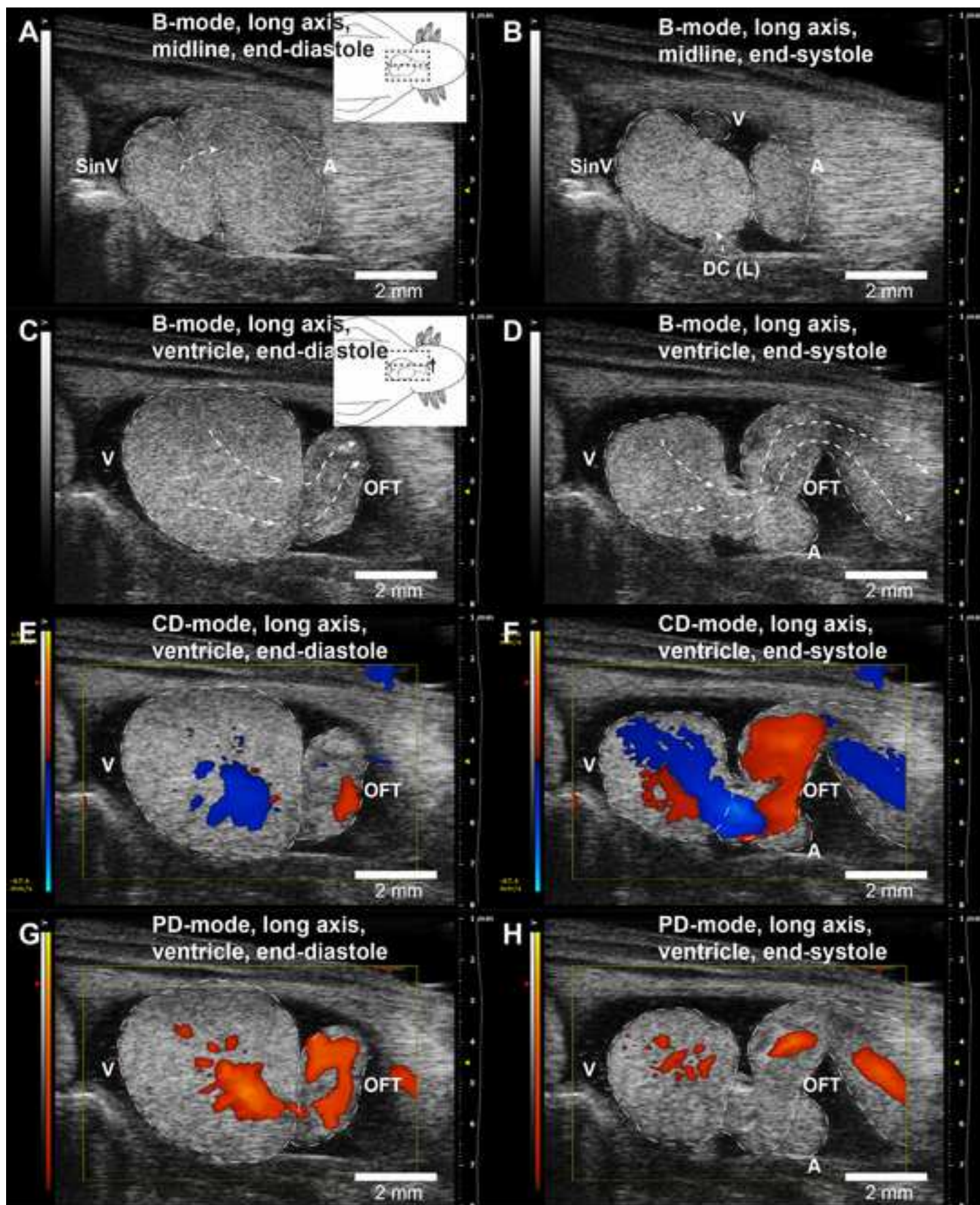
- 827  
828 13. Gressens, J. An introduction to the Mexican axolotl (*Ambystoma mexicanum*). *Lab Animal*  
829 **33**, 41-47 (2004).  
830
- 831 14. Cano-Martínez, A., Vargas-González, A., Guarner-Lans, V., Prado-Zayago, E., León-Oleda,  
832 M., Nieto-Lima, B. Functional and structural regeneration in the axolotl heart (*Ambystoma*  
833 *mexicanum*) after partial ventricular amputation. *Arch. Cardiol. Mex.* **80**, 79–86 (2010).  
834
- 835 15. McCusker, C., Gardiner, D.M. The axolotl model for regeneration and aging research: a  
836 mini-review. *Gerontology* **57**, 565-571 (2011).  
837
- 838 16. Khattak, S. et al. Optimized axolotl (*Ambystoma mexicanum*) husbandry, breeding,  
839 metamorphosis, transgenesis and tamoxifen-mediated recombination. *Nat. Protoc.* **9**, 529-540  
840 (2014).  
841
- 842 17. Nakamura, R. et al. Expression analysis of Baf60c during heart regeneration in axolotls  
843 and neonatal mice. *Develop. Growth Differ.* **58**, 367-382 (2016)  
844
- 845
- 846 18. Tan, G.X.Y., Jamil, M., Tee, N.G.Z., Zhong, L., Yap, C.H. 3D Reconstruction of Chick Embryo  
847 Vascular Geometry Using Non-Invasive High-Frequency Ultrasound for Computational Fluid  
848 Dynamics. *Ann. Biomed. Eng.* **43**, 2780-2793 (2015).  
849
- 850 19. Ho, S., Tan, G.X.Y., Foo, T.J., Phan-Thien, N., Yap, C.H. Organ Dynamics and Fluid Dynamics  
851 of the HH25 Chick Embryonic Cardiac Ventricle as Revealed by a Novel 4D High-Frequency  
852 Ultrasound Imaging Technique and Computational Flow Simulations. *Ann. Biomed. Eng.* doi:  
853 10.1007/s10439-017-1882-9. [Epub ahead of print] (2017).  
854
- 855 20. Wasmeier, G.H., et al. Reproducibility of transthoracic echocardiography in small animals  
856 using clinical equipment. *Coron. Artery. Dis.* **18**, 283-291 (2007).  
857
- 858 21. Thygesen, M.M., Rasmussen, M.M., Madsen, J.G., Pedersen, M. and Lauridsen, H.  
859 Propofol (2,6-diisopropylphenol) is an applicable immersion anesthetic in the axolotl with  
860 potential uses in hemodynamic and neurophysiological experiments. *Regeneration* **0**, 1–9,  
861 <https://doi.org/10.1002/reg2.80> (2017).  
862

Figure 1

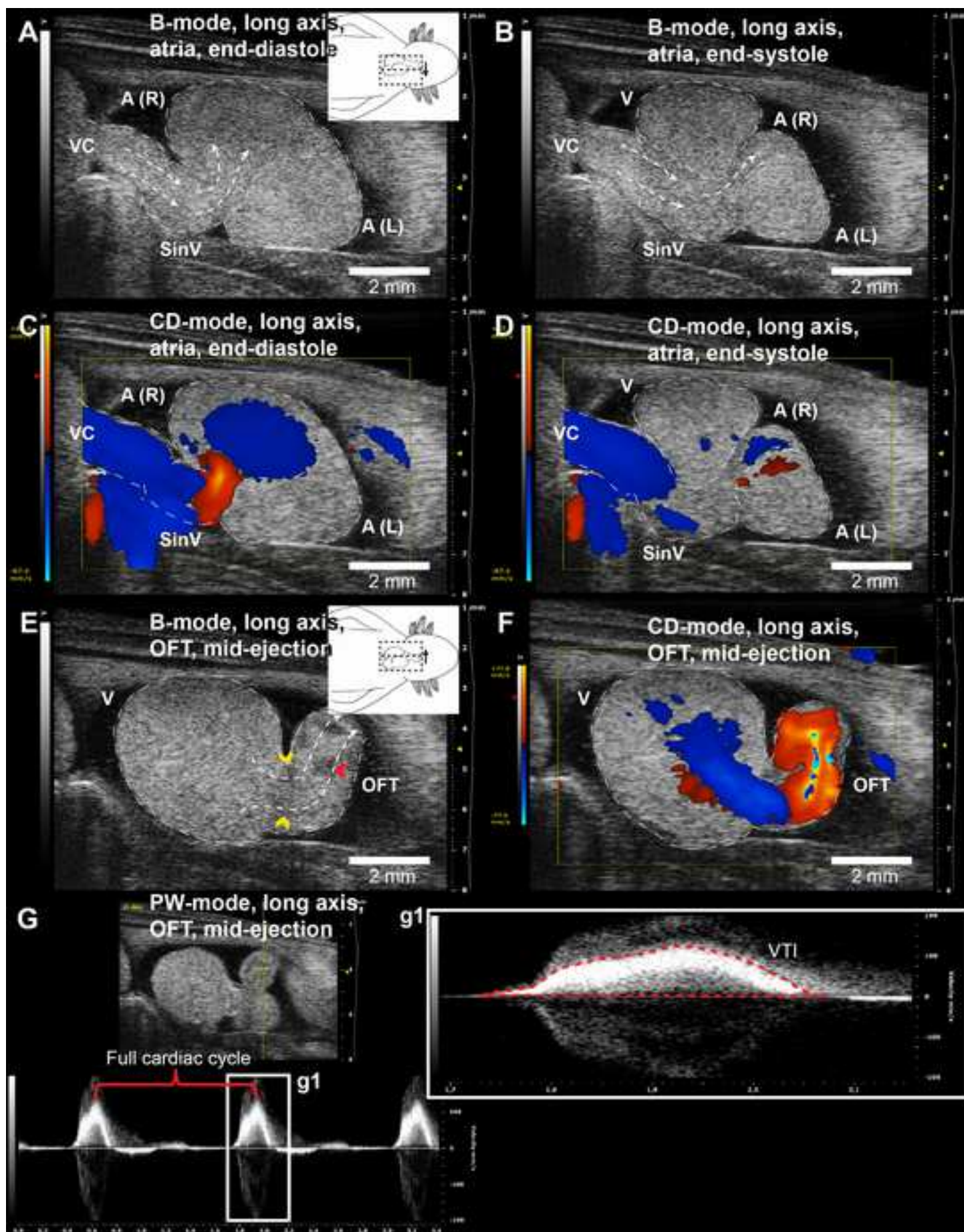


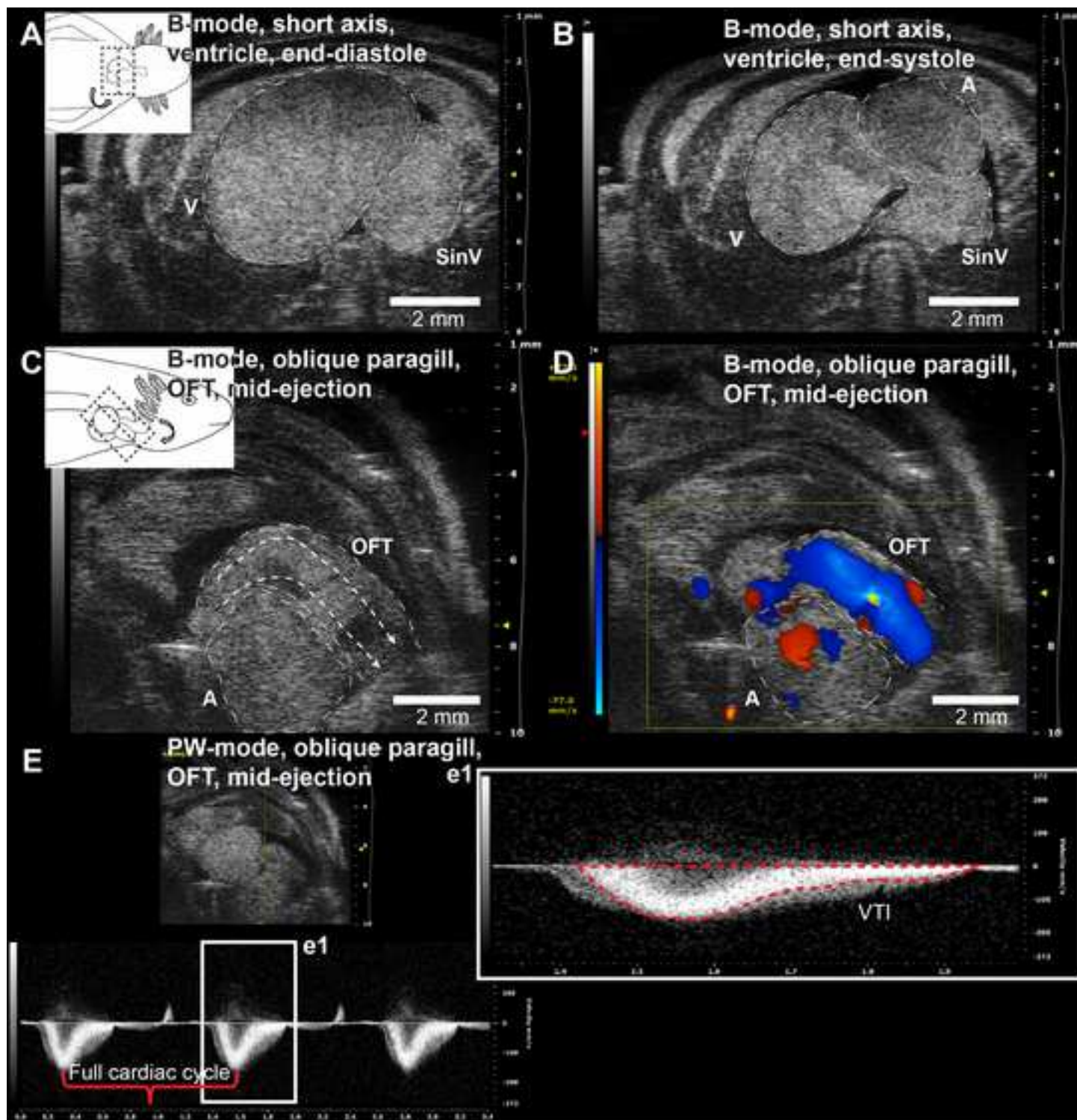




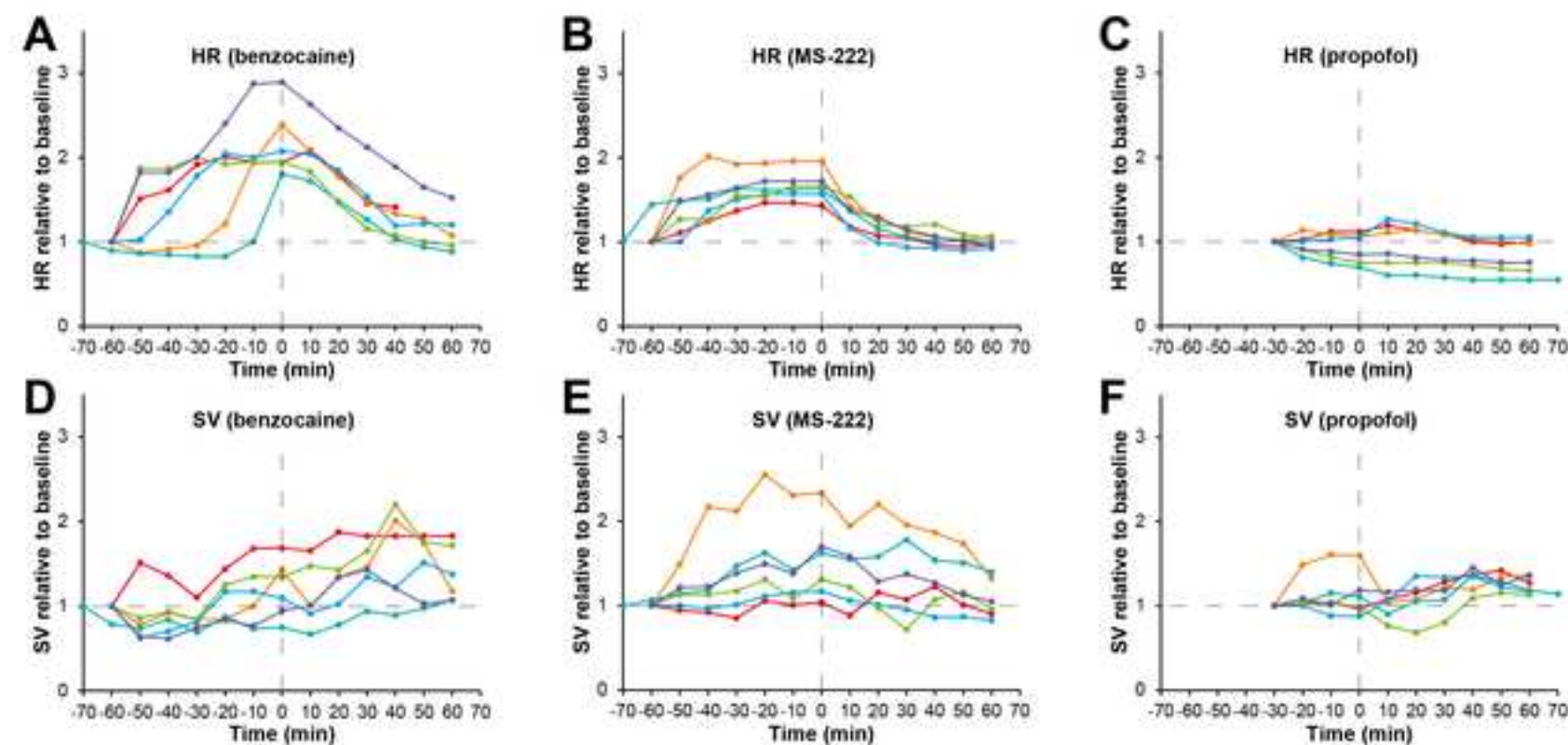




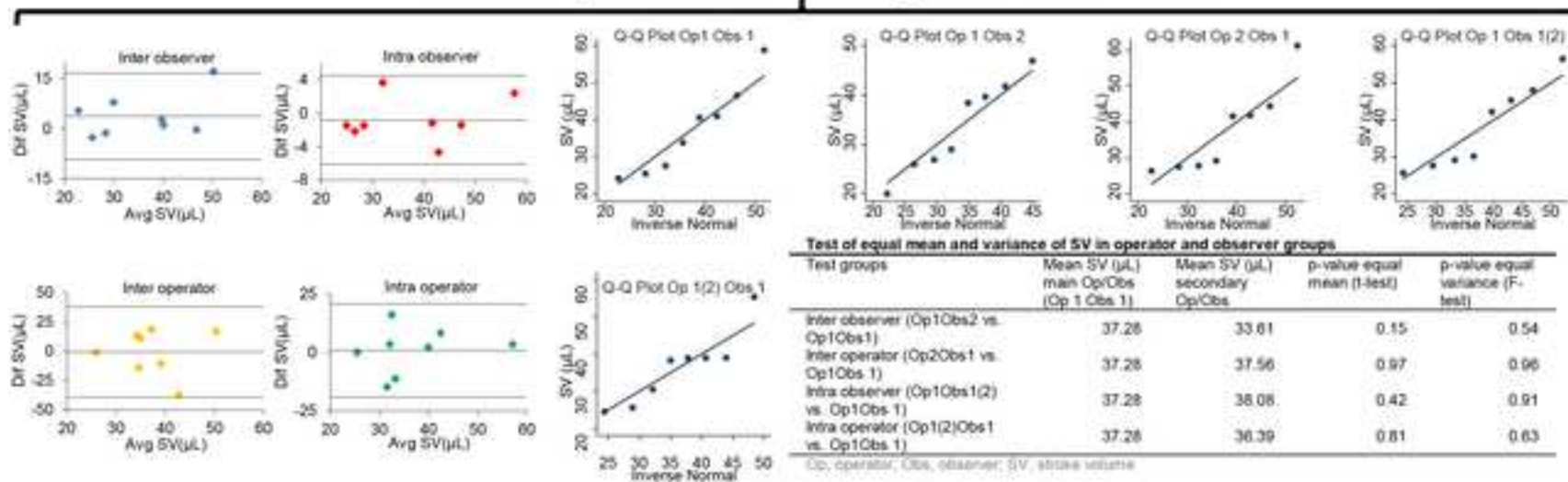


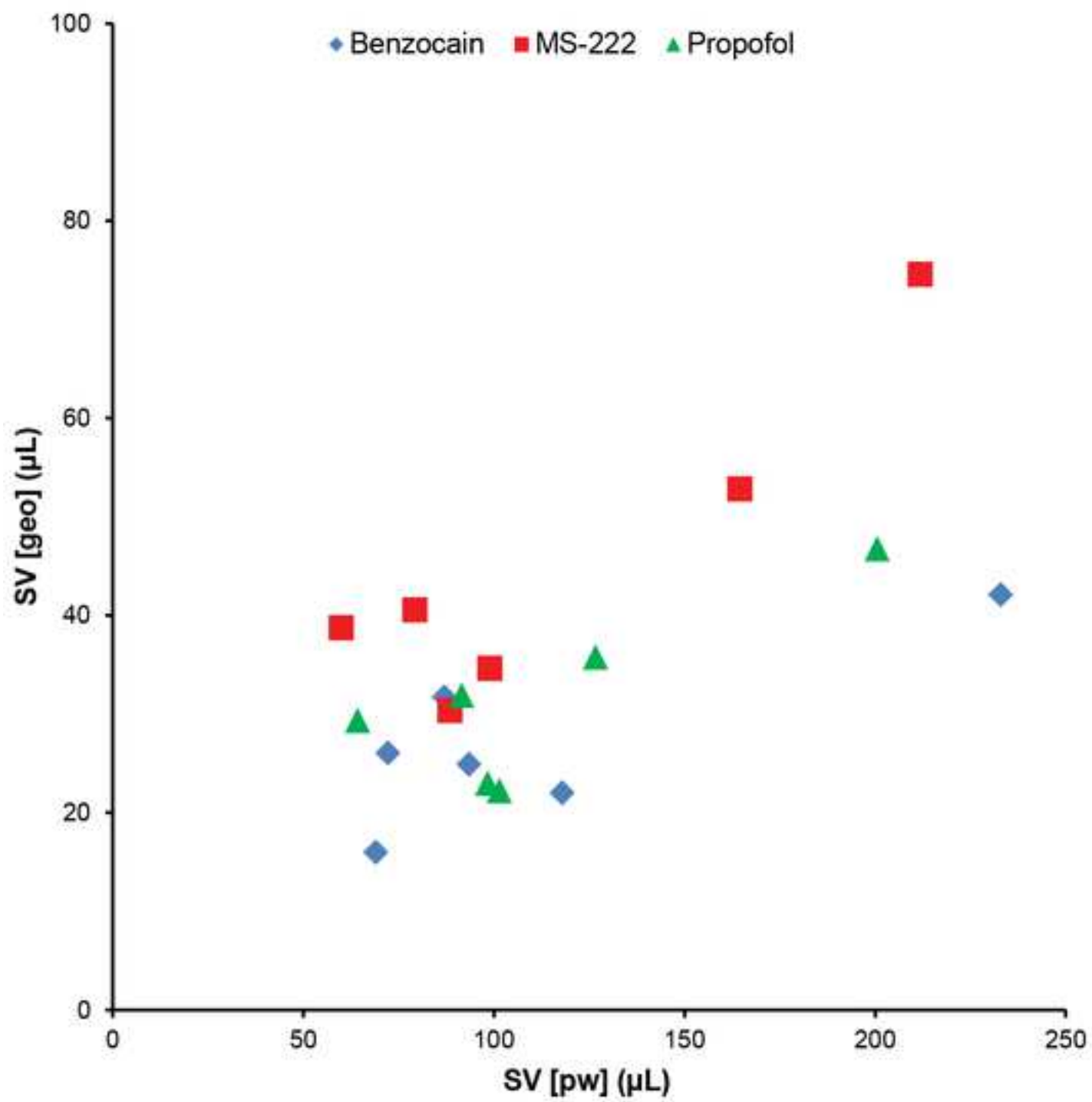






## G Intra/inter-operator/observer analysis on stroke volume





[Click here to download Figure Fig\\_8.tif](#) 

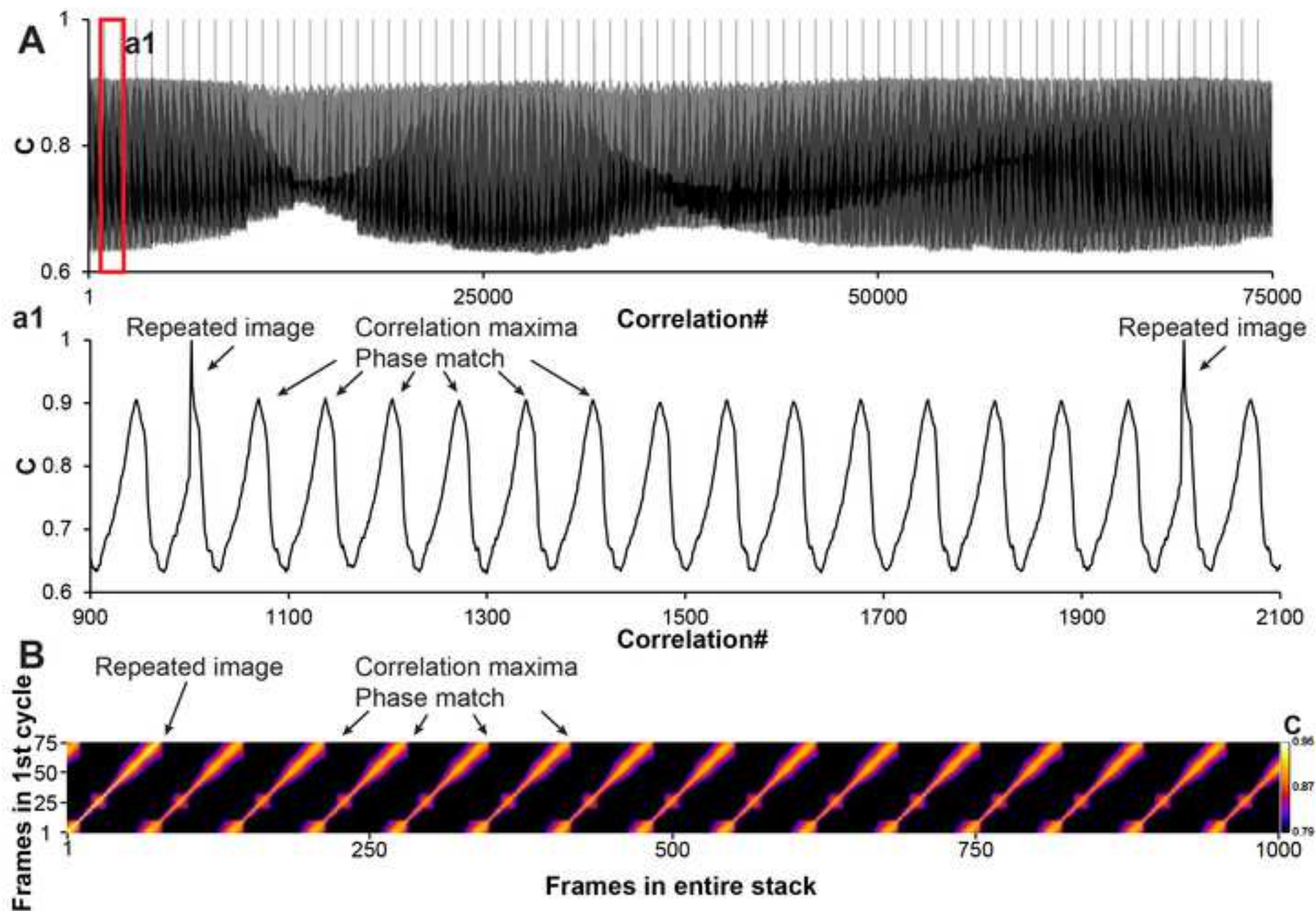
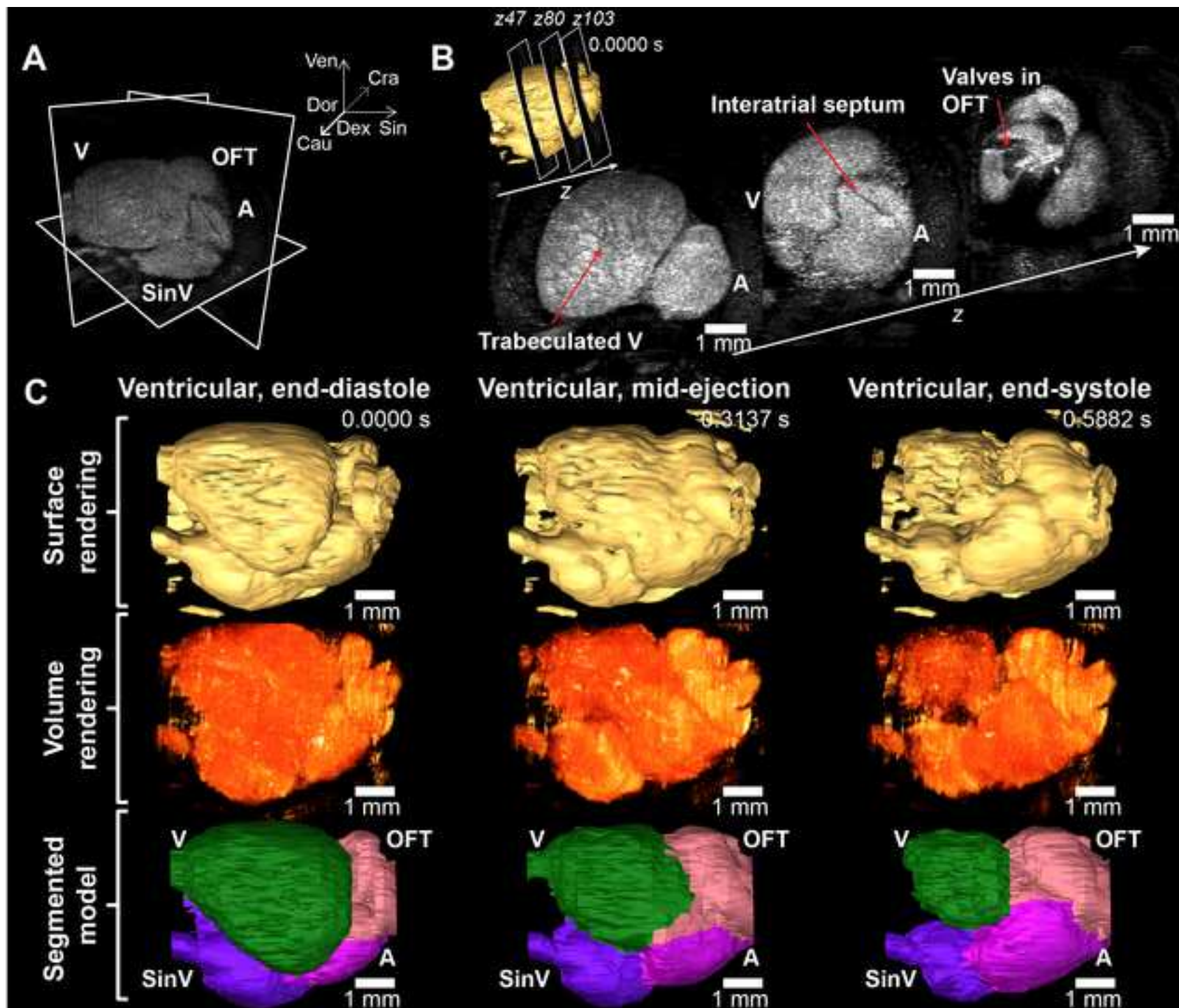




Figure 9





Name of Material/ Equipment	Company	Catalog Number
Axolotl (Ambystoma mexicanum)	Exoterra GmbH	N/A
Vevo 2100	Fujifilm, Visualsonics	Vevo 2100
MS700	Fujifilm, Visualsonics	MS700
MS550s	Fujifilm, Visualsonics	MS550s
Micromanipulator	Zeiss	NA
Benzocain	Sigma-Aldrich	94-09-7
MS-222	Sigma-Aldrich	886-86-2
Propofol	B. Braun Medical A/S	NA
Sodium chloride	Sigma-Aldrich	7647-14-5
Calcium chloride dihydrate	Sigma-Aldrich	10035-04-8
Magnesium sulfate heptahydrate	Sigma-Aldrich	10034-99-8
Potassium chloride	Sigma-Aldrich	7447-40-7
Acetone	Sigma-Aldrich	67-64-1
Soft cloth	N/A	N/A
Styrofoam block	N/A	N/A
Plastic wrap	N/A	N/A
Tape	BSN Medical	72359-02
Kimwipes	Sigma-Aldrich	Z188956
Excel 2010	Microsoft	N/A
ImageJ	National Institutes of Health	

### Comments/Description

All strains (wildtype, melanoid, white, albino, transgenic white with GFP) can be applied for echocardiography

High frequency ultrasound system

50 MHz center frequency, transducer

40 MHz center frequency, transducer

ethyl 4-aminobenzoate

ethyl 3-aminobenzoate methanesulfonic acid

2,6-diisopropylphenol

NaCl

$\text{CaCl}_2 \cdot 2\text{H}_2\text{O}$

$\text{MgSO}_4 \cdot 7\text{H}_2\text{O}$

KCl

Propanone

Any piece of soft cloth measuring approximately  $70 \times 55 \text{ cm}^2$  e.g. a dish towel

Any piece of Styrofoam block measuring approximately  $33 \times 27 \times 5 \text{ cm}^3$  e.g. a medium sized Styrofoam cooler lid

Any piece of plastic wrap e.g. food wrap

Leukoplast sleek

Kimwipes, disposable wipers

Excel 2010 or newer

ImageJ 1.5e or newer. Rasband, W.S., ImageJ, U. S. National Institutes of Health, Bethesda, Maryland, USA, <https://imagej.nih.gov/ij/>, 19

197-2016.



1 Alewife Center #200  
Cambridge, MA 02140  
tel. 617.945.9051  
www.jove.com

## ARTICLE AND VIDEO LICENSE AGREEMENT

Title of Article: 2D and 3D echocardiography in the axolotl (*Ambystoma mexicanum*)  
Author(s): Anita Dittrich, Mathias Møller Thygesen, Henrik Lauridsen

Item 1 (check one box): The Author elects to have the Materials be made available (as described at <http://www.jove.com/author>) via: ☒ Standard Access ☐ Open Access

Item 2 (check one box):

- ☒ The Author is NOT a United States government employee.
- ☐ The Author is a United States government employee and the Materials were prepared in the course of his or her duties as a United States government employee.
- ☐ The Author is a United States government employee but the Materials were NOT prepared in the course of his or her duties as a United States government employee.

### ARTICLE AND VIDEO LICENSE AGREEMENT

1. **Defined Terms.** As used in this Article and Video License Agreement, the following terms shall have the following meanings: “**Agreement**” means this Article and Video License Agreement; “**Article**” means the article specified on the last page of this Agreement, including any associated materials such as texts, figures, tables, artwork, abstracts, or summaries contained therein; “**Author**” means the author who is a signatory to this Agreement; “**Collective Work**” means a work, such as a periodical issue, anthology or encyclopedia, in which the Materials in their entirety in unmodified form, along with a number of other contributions, constituting separate and independent works in themselves, are assembled into a collective whole; “**CRC License**” means the Creative Commons Attribution-Non Commercial-No Derivs 3.0 Unported Agreement, the terms and conditions of which can be found at: <http://creativecommons.org/licenses/by-nc-nd/3.0/legalcode>; “**Derivative Work**” means a work based upon the Materials or upon the Materials and other pre-existing works, such as a translation, musical arrangement, dramatization, fictionalization, motion picture version, sound recording, art reproduction, abridgment, condensation, or any other form in which the Materials may be recast, transformed, or adapted; “**Institution**” means the institution, listed on the last page of this Agreement, by which the Author was employed at the time of the creation of the Materials; “**JoVE**” means MyJoVE Corporation, a Massachusetts corporation and the publisher of *The Journal of Visualized Experiments*; “**Materials**” means the Article and / or the Video; “**Parties**” means the Author and JoVE; “**Video**” means any video(s) made by the Author, alone or in conjunction with any other parties, or by JoVE or its affiliates or agents, individually or in collaboration with the Author or any other parties, incorporating all or any portion of the Article, and in which the Author may or may not appear.

2. **Background.** The Author, who is the author of the Article, in order to ensure the dissemination and protection of the Article, desires to have the JoVE publish the Article and create and transmit videos based on the Article. In furtherance of such goals, the Parties desire to memorialize in this Agreement the respective rights of each Party in and to the Article and the Video.

3. **Grant of Rights in Article.** In consideration of JoVE agreeing to publish the Article, the Author hereby grants to JoVE, subject to **Sections 4** and **7** below, the exclusive, royalty-free, perpetual (for the full term of copyright in the Article, including any extensions thereto) license (a) to publish, reproduce, distribute, display and store the Article in all forms, formats and media whether now known or hereafter developed (including without limitation in print, digital and electronic form) throughout the world, (b) to translate the Article into other languages, create adaptations, summaries or extracts of the Article or other Derivative Works (including, without limitation, the Video) or Collective Works based on all or any portion of the Article and exercise all of the rights set forth in (a) above in such translations, adaptations, summaries, extracts, Derivative Works or Collective Works and (c) to license others to do any or all of the above. The foregoing rights may be exercised in all media and formats, whether now known or hereafter devised, and include the right to make such modifications as are technically necessary to exercise the rights in other media and formats. If the “Open Access” box has been checked in **Item 1** above, JoVE and the Author hereby grant to the public all such rights in the Article as provided in, but subject to all limitations and requirements set forth in, the CRC License.

## ARTICLE AND VIDEO LICENSE AGREEMENT

4. Retention of Rights in Article. Notwithstanding the exclusive license granted to JoVE in **Section 3** above, the Author shall, with respect to the Article, retain the non-exclusive right to use all or part of the Article for the non-commercial purpose of giving lectures, presentations or teaching classes, and to post a copy of the Article on the Institution's website or the Author's personal website, in each case provided that a link to the Article on the JoVE website is provided and notice of JoVE's copyright in the Article is included. All non-copyright intellectual property rights in and to the Article, such as patent rights, shall remain with the Author.

5. Grant of Rights in Video – Standard Access. This **Section 5** applies if the "Standard Access" box has been checked in **Item 1** above or if no box has been checked in **Item 1** above. In consideration of JoVE agreeing to produce, display or otherwise assist with the Video, the Author hereby acknowledges and agrees that, Subject to **Section 7** below, JoVE is and shall be the sole and exclusive owner of all rights of any nature, including, without limitation, all copyrights, in and to the Video. To the extent that, by law, the Author is deemed, now or at any time in the future, to have any rights of any nature in or to the Video, the Author hereby disclaims all such rights and transfers all such rights to JoVE.

6. Grant of Rights in Video – Open Access. This **Section 6** applies only if the "Open Access" box has been checked in **Item 1** above. In consideration of JoVE agreeing to produce, display or otherwise assist with the Video, the Author hereby grants to JoVE, subject to **Section 7** below, the exclusive, royalty-free, perpetual (for the full term of copyright in the Article, including any extensions thereto) license (a) to publish, reproduce, distribute, display and store the Video in all forms, formats and media whether now known or hereafter developed (including without limitation in print, digital and electronic form) throughout the world, (b) to translate the Video into other languages, create adaptations, summaries or extracts of the Video or other Derivative Works or Collective Works based on all or any portion of the Video and exercise all of the rights set forth in (a) above in such translations, adaptations, summaries, extracts, Derivative Works or Collective Works and (c) to license others to do any or all of the above. The foregoing rights may be exercised in all media and formats, whether now known or hereafter devised, and include the right to make such modifications as are technically necessary to exercise the rights in other media and formats. For any Video to which this Section 6 is applicable, JoVE and the Author hereby grant to the public all such rights in the Video as provided in, but subject to all limitations and requirements set forth in, the CRC License.

7. Government Employees. If the Author is a United States government employee and the Article was prepared in the course of his or her duties as a United States government employee, as indicated in **Item 2** above, and any of the licenses or grants granted by the Author hereunder exceed the scope of the 17 U.S.C. 403, then the rights granted hereunder shall be limited to the maximum rights permitted under such

statute. In such case, all provisions contained herein that are not in conflict with such statute shall remain in full force and effect, and all provisions contained herein that do so conflict shall be deemed to be amended so as to provide to JoVE the maximum rights permissible within such statute.

8. Likeness, Privacy, Personality. The Author hereby grants JoVE the right to use the Author's name, voice, likeness, picture, photograph, image, biography and performance in any way, commercial or otherwise, in connection with the Materials and the sale, promotion and distribution thereof. The Author hereby waives any and all rights he or she may have, relating to his or her appearance in the Video or otherwise relating to the Materials, under all applicable privacy, likeness, personality or similar laws.

9. Author Warranties. The Author represents and warrants that the Article is original, that it has not been published, that the copyright interest is owned by the Author (or, if more than one author is listed at the beginning of this Agreement, by such authors collectively) and has not been assigned, licensed, or otherwise transferred to any other party. The Author represents and warrants that the author(s) listed at the top of this Agreement are the only authors of the Materials. If more than one author is listed at the top of this Agreement and if any such author has not entered into a separate Article and Video License Agreement with JoVE relating to the Materials, the Author represents and warrants that the Author has been authorized by each of the other such authors to execute this Agreement on his or her behalf and to bind him or her with respect to the terms of this Agreement as if each of them had been a party hereto as an Author. The Author warrants that the use, reproduction, distribution, public or private performance or display, and/or modification of all or any portion of the Materials does not and will not violate, infringe and/or misappropriate the patent, trademark, intellectual property or other rights of any third party. The Author represents and warrants that it has and will continue to comply with all government, institutional and other regulations, including, without limitation all institutional, laboratory, hospital, ethical, human and animal treatment, privacy, and all other rules, regulations, laws, procedures or guidelines, applicable to the Materials, and that all research involving human and animal subjects has been approved by the Author's relevant institutional review board.

10. JoVE Discretion. If the Author requests the assistance of JoVE in producing the Video in the Author's facility, the Author shall ensure that the presence of JoVE employees, agents or independent contractors is in accordance with the relevant regulations of the Author's institution. If more than one author is listed at the beginning of this Agreement, JoVE may, in its sole discretion, elect not take any action with respect to the Article until such time as it has received complete, executed Article and Video License Agreements from each such author. JoVE reserves the right, in its absolute and sole discretion and without giving any reason therefore, to accept or decline any work submitted to JoVE. JoVE and its employees, agents and independent contractors shall have

## ARTICLE AND VIDEO LICENSE AGREEMENT

full, unfettered access to the facilities of the Author or of the Author's institution as necessary to make the Video, whether actually published or not. JoVE has sole discretion as to the method of making and publishing the Materials, including, without limitation, to all decisions regarding editing, lighting, filming, timing of publication, if any, length, quality, content and the like.

11. Indemnification. The Author agrees to indemnify JoVE and/or its successors and assigns from and against any and all claims, costs, and expenses, including attorney's fees, arising out of any breach of any warranty or other representations contained herein. The Author further agrees to indemnify and hold harmless JoVE from and against any and all claims, costs, and expenses, including attorney's fees, resulting from the breach by the Author of any representation or warranty contained herein or from allegations or instances of violation of intellectual property rights, damage to the Author's or the Author's institution's facilities, fraud, libel, defamation, research, equipment, experiments, property damage, personal injury, violations of institutional, laboratory, hospital, ethical, human and animal treatment, privacy or other rules, regulations, laws, procedures or guidelines, liabilities and other losses or damages related in any way to the submission of work to JoVE, making of videos by JoVE, or publication in JoVE or elsewhere by JoVE. The Author shall be responsible for, and shall hold JoVE harmless from, damages caused by lack of sterilization, lack of cleanliness or by contamination due to the making of a video by JoVE its employees, agents or independent contractors. All sterilization, cleanliness or decontamination procedures shall be solely the responsibility of the Author and shall be undertaken at the Author's


expense. All indemnifications provided herein shall include JoVE's attorney's fees and costs related to said losses or damages. Such indemnification and holding harmless shall include such losses or damages incurred by, or in connection with, acts or omissions of JoVE, its employees, agents or independent contractors.

12. Fees. To cover the cost incurred for publication, JoVE must receive payment before production and publication the Materials. Payment is due in 21 days of invoice. Should the Materials not be published due to an editorial or production decision, these funds will be returned to the Author. Withdrawal by the Author of any submitted Materials after final peer review approval will result in a US\$1,200 fee to cover pre-production expenses incurred by JoVE. If payment is not received by the completion of filming, production and publication of the Materials will be suspended until payment is received.

13. Transfer, Governing Law. This Agreement may be assigned by JoVE and shall inure to the benefits of any of JoVE's successors and assignees. This Agreement shall be governed and construed by the internal laws of the Commonwealth of Massachusetts without giving effect to any conflict of law provision thereunder. This Agreement may be executed in counterparts, each of which shall be deemed an original, but all of which together shall be deemed to be one and the same agreement. A signed copy of this Agreement delivered by facsimile, e-mail or other means of electronic transmission shall be deemed to have the same legal effect as delivery of an original signed copy of this Agreement.

A signed copy of this document must be sent with all new submissions. Only one Agreement required per submission.

### CORRESPONDING AUTHOR:

Name:	Henrik Lauridsen	
Department:	Department of Clinical Medicine	
Institution:	Aarhus University	
Article Title:	2D and 3D echocardiography in the axolotl ( <i>Ambystoma mexicanum</i> )	
Signature:		Date: July 31, 2017

Please submit a signed and dated copy of this license by one of the following three methods:

- 1) Upload a scanned copy of the document as a pdf on the JoVE submission site;
- 2) Fax the document to +1.866.381.2236;
- 3) Mail the document to JoVE / Attn: JoVE Editorial / 1 Alewife Center #200 / Cambridge, MA 02139

For questions, please email [submissions@jove.com](mailto:submissions@jove.com) or call +1.617.945.9051

First of all we would like to take the opportunity to thank the editor and five reviewers for providing thorough reviews of our paper. It is a pleasure to see that both editor and reviewers have been going into detail in the evaluation of the manuscript and provide excellent comments and thoughts for the improvement of the manuscript. In the following we try to answer the comments/questions raised by the editor and reviewers (response in red) and describe how their suggestions have been incorporated into the revised manuscript (line numbers refer to the revised manuscript with track changes enabled).

### **Changes recommended by the JoVE Scientific Review Editor:**

- Please take this opportunity to thoroughly proofread the manuscript to ensure that there are no spelling or grammatical errors.

We have thoroughly proofread the manuscript and corrected for spelling and grammatical errors.

- Protocol Language: Please ensure that ALL text in the protocol section is written in the imperative tense as if you are telling someone how to do the technique (i.e. “Do this”, “Measure that” etc.) Any text that cannot be written in the imperative tense may be added as a “Note”, however, notes should be used sparingly and actions should be described in the imperative tense wherever possible.

1) Examples NOT in imperative tense: “High quality non-chemically treated tap water can be applied directly.”; “The lip shaped structure can be submerged...”; “General anesthesia will appear within 30 min in all size groups for both benzocaine”; entire section 5.

Protocol text has been rephrased so all text (except that in notes) is in the imperative tense.

- Protocol Detail: Please note that your protocol will be used to generate the script for the video, and must contain everything that you would like shown in the video. Please ensure you answer the “how” question, i.e., how is the step performed? Alternatively, for steps that will not be filmed, add references to published material specifying how to perform the protocol action. There should be enough detail in each step to supplement the actions seen in the video so that viewers can easily replicate the protocol. Some examples:

1) For all software steps: Please mention what button is clicked on in the software, or which menu items need to be selected to perform the step.

This is tricky. The software steps described in the protocol are too complex to be described as “click that button”, “open that menu” etc. That would require thousands of steps. Instead we believe the best way to describe the software procedures are to present the math underlying the procedures in the protocol steps and supply the reader with supplementary material (Supplementary material 16 – 20) containing

pre-written scripts for software that most researches within biomedical research will be familiar with (Excel and ImageJ)

- Protocol Highlight: After you have made all of the recommended changes to your protocol (listed above), please re-evaluate the length of your protocol section. There is a 10-page limit for the protocol text, and a 3- page limit for filmable content. If your protocol is longer than 3 pages, please highlight ~2.5 pages or less of text (which includes headings and spaces) in yellow, to identify which steps should be visualized to tell the most cohesive story of your protocol steps.

- o The highlighting must include all relevant details that are required to perform the step. For example, if step 2.5 is highlighted for filming and the details of how to perform the step are given in steps 2.5.1 and 2.5.2, then the sub-steps where the details are provided must be included in the highlighting.

- o The highlighted steps should form a cohesive narrative, that is, there must be a logical flow from one highlighted step to the next.

- o Please highlight complete sentences (not parts of sentences). Include sub-headings and spaces when calculating the final highlighted length.

- o Notes cannot be filmed and should be excluded from highlighting.

- o Please bear in mind that software steps without a graphical user interface/calculations cannot be filmed.

We have evaluated the length of the protocol and it is below the 10 pages limit. We have highlighted <2.5 pages that tell a cohesive story of our protocol steps and should be visualized.

- Discussion: JoVE articles are focused on the methods and the protocol, thus the discussion should be similarly focused. Please ensure that the discussion covers the following in detail and in paragraph form: 1) modifications and troubleshooting, 2) limitations of the technique, 3) significance with respect to existing methods, 4) future applications and 5) critical steps within the protocol.

We believe that the discussion covers these subjects.

- Commercial Language: JoVE is unable to publish manuscripts containing commercial sounding language, including trademark or registered trademark symbols (TM/R) and the mention of company brand names before an instrument or reagent. Examples of commercial sounding language in your manuscript are Milli-Q, Styrofoam, kimwipes, Vevo 2100, etc

- 1) Please use MS Word's find function (Ctrl+F), to locate and replace all commercial sounding language in your manuscript with generic names that are not company-specific. All commercial products should



be sufficiently referenced in the table of materials/reagents. You may use the generic term followed by “(see table of materials)” to draw the readers’ attention to specific commercial names.

Commercial names have been replaced by generic names.

- Table of Materials: Please revise the table of the essential supplies, reagents, and equipment. The table should include the name, company, and catalog number of all relevant materials/software in separate columns in an xls/xlsx file. Please include items such as axolotl strain, software, imagers, etc.

Table of Materials has been updated.

- Please define all abbreviations at first use.

We believe that all abbreviations are defined at first use.

- Please use standard abbreviations and symbols for SI Units such as  $\mu\text{L}$ , mL, L, etc., and abbreviations for non-SI units such as h, min, s for time units. Please use a single space between the numerical value and unit.

We believe that all units are in SI units with correct abbreviations.

- If your figures and tables are original and not published previously or you have already obtained figure permissions, please ignore this comment. If you are re-using figures from a previous publication, you must obtain explicit permission to re-use the figure from the previous publisher (this can be in the form of a letter from an editor or a link to the editorial policies that allows you to re-publish the figure). Please upload the text of the re-print permission (may be copied and pasted from an email/website) as a Word document to the Editorial Manager site in the "Supplemental files (as requested by JoVE)" section. Please also cite the figure appropriately in the figure legend, i.e. "This figure has been modified from [citation]."

We reuse material from one of our own previous publications (Thygesen, M.M., Rasmussen, M.M., Madsen, J.G., Pedersen, M. and Lauridsen, H. Propofol (2,6-diisopropylphenol) is an applicable immersion anesthetic in the axolotl with potential uses in hemodynamic and neurophysiological experiments. *Regeneration* 0, 1–9, <https://doi.org/10.1002/reg2.80> (2017)). Since this material is available under the Creative Commons Attribution License we believe that permission is not required for academic or commercial reuse, provided that full attribution is included in the new work. This is also specified on the publisher’s homepage: [http://onlinelibrary.wiley.com/journal/10.1002/\(ISSN\)2052-4412/homepage/Permissions.html](http://onlinelibrary.wiley.com/journal/10.1002/(ISSN)2052-4412/homepage/Permissions.html)

## **Comments from Peer-Reviewers:**

### **Reviewer #1:**

#### Manuscript Summary:

The protocol describes several different methods to acquire echocardiographic measurements on the axolotl heart in anesthetized and unanesthetized animals in two and three spatial dimensions. The authors assessed three different anesthetics: benzocaine, trichaine, and propofol. The methods are applicable in heart regenerative experiments where cardiac function can be monitored over the course of a regeneration process. Moreover, the method could be useful for cardophysiological studies in different experimental conditions.

#### Major Concerns:

None

#### Minor Concerns:

None

### **Reviewer #2:**

#### Manuscript Summary:

The manuscript by Dittrich et al provides a thorough protocol for the visualization of the axolotl heart by echocardiography. The axolotl is an interesting choice of animal due to its regenerative capacity, and the authors correctly argue that similar studies are currently lacking from the literature. Successful visualizations by echocardiography at times require subtle approaches which are not easily described in words, but may be very well visualized on video. JoVE seems to be a wholly appropriate outlet for the submitted protocol. I have no major concerns with the manuscript. The text is concise and exhaustive, the figures are good.

#### Minor Concerns:

Besides a number of specific comments, please see below, I only have one general comment. Line 705-706: what to make of the discrepancy between the values derived from Doppler and those derived from

the equation assuming a spherical ventricle? It would be nice to see a comparison between the values, for instance a simple scatter plot with stroke volume assuming a sphere versus stroke volume measured by Doppler. Did you attempt to quantify by Doppler cardiac output as flow through the atrioventricular canal? If so, the relation between the cardiac output as assessed from the atrioventricular canal and the outflow tract could be used to the reliability of stroke volume as derived from the equation assuming a spherical ventricle.

We have made a scatterplot (Fig. 7) showing stroke volume values acquired by the geometrical equation and the Doppler method for all three anesthetics described in the study (benzocaine, MS-222, and propofol). We haven't attempted to quantify Doppler cardiac output as flow through the atrioventricular canal.

Specific comments

With the described setup, can the echocardiography be synchronized with electrocardiograms?

We have attempted to synchronize echocardiography with electrocardiograms previously, but haven't been successful, hence we have not included any comments regarding this in the manuscript.

The literature on Axolotl regeneration is well cited, but you may also be interested in the recent study by Nakamura et al in Development, Growth & Differentiation 58, no. 4 (2016): 367-382.

This is a relevant paper and we have referenced it in the revised manuscript (l. 64 and l. 836-837).

Line 21: try to avoid that the verbs are placed at the end of the sentence

We are not sure what the reviewer is getting at here. We cannot find any verbs in original line 21 ("Long abstract") and cannot find examples of verbs placed at the end of sentences in the adjacent sentences.

Line 29: "to meaningfully and reproducibly" - reproducible is good enough. I suggest to leave it to your readers whether something is meaningful.

We agree and have left out "meaningfully" (l. 29 and l. 70).

Line 32: "Due to the lack in dimensionality, " I don't think this sentence makes sense, and it can be deleted without the loss of any meaning.

Sentence has been deleted (l. 32-33).

Line 52-55: this sentence is redundant

We disagree and are inclined to leave the sentence. We believe it is important to introduce the zebrafish as an important model in heart regeneration but also put emphasis on both pros and cons in this model in order to justify the use of a larger model like the axolotl.

Line 60: delete "to be"

"to be" is deleted (l. 61.)

Line 163-164: "Ensure positioning of cranial to the right" - why?

This is the traditional practice in echocardiography and ensures standardized acquisitions that are easy to interpret for other. We have extended the sentence to clarify this (l. 178).

Line 185: how much does the ventricle approximate the spherical shape? Consider on the basis of this recent paper whether there should adjustments to your assumption of complete sphericity: Perrichon, Prescilla, Martin Grosell, and Warren W. Burggren. "Heart Performance Determination by Visualization in Larval Fishes: Influence of Alternative Models for Heart Shape and Volume." *Frontiers in Physiology* 8 (2017).

This is a very interesting paper. The best evidence that the spherical assumption is not perfect comes from our own 3D data (Supplementary material 13-15). Especially in the end-diastolic phase the spherical assumption is not exactly accurate. But we do believe that the spherical model is reasonable to use for its simplicity, though a better model encompassing different life stages and sizes of the axolotl would be interesting to develop as derivative work.

Line 294: haunted is an odd choice of word

Sentence has been rewritten and "haunted" left out (l. 307-310).

Line 703-704: "Likewise, echocardiographic measurements should be viewed more as index values rather than absolute values." Indexed to what? In cardiology, functional measures are typically indexed to body mass or the calculated body surface, but this has nothing to do with the reproducibility of the primary data and instead concerns comparisons between individuals.

Our use of index is in the meaning of something that serves to guide, point out, or otherwise facilitate reference between measurements made under different circumstances, i.e. values that can be used to study relative changes. We have tried to highlight that point in the new version of the sentence (l. 734-735).

### **Reviewer #3:**

Manuscript Summary:

The focus of the current manuscript is to exhibit different methods of measuring cardiac function in the Mexican Axolotl. This is a powerful model to study regenerative processes, such as heart regeneration, and the authors speculate that these protocols will be useful in making measurements on regenerating axolotl hearts in the future. The authors discuss how different methods of anesthesia are used on the axolotl in addition to 2D echocardiography (in anesthetized and unanesthetized animals), how to evaluate 2D echocardiography, and 3D echocardiography. The representative data seems appropriate and the protocols appear to have all of the appropriate details to perform similar experiments -however

since this technology is outside of my realm of expertise, I can't be sure that sufficient detail is provided. I think that the protocols provided here will be useful to those that study cardiac function and regeneration in axolotl.

#### Minor Concerns:

1) Figures are referenced in text out of order. For example, figure 6 is referenced before figure 2. It is common practice to have figures numbered in the order that they are referenced in the text.

We agree with the reviewer. The reason is the multifaceted nature of the figures that makes it very difficult both to combine different representative results in appealing figures and still strictly adhere to the order of the figures when presenting them in the text. We have now initially introduced all the figures in the introduction in such way the later referencing to specific figures can follow the logic of the text (l. 69 – 72).

2) For individuals that are not familiar with making measurements on cardiac function -explaining a little more on axolotl cardiac anatomy, and what exactly is being measured with an echocardiograph, would be very helpful. I think that adding this to the introduction makes the most sense.

We have added a more in-depth description of cardiac anatomy in the axolotl (amphibians in general) to the introduction (l. 72-76). We prefer to leave out a very general introduction to echocardiography/ultrasound imaging from the manuscript since this is widely available information in textbooks and imaging courses.

3) In Figure 3, the insets of the images of the axolotl are very hard to see. I would either make a larger version of these, or draw a simple cartoon with the appropriate positions indicated.

We agree with the reviewer that these photos were hard to see. We have instead inserted simple cartoon drawings as suggested (Fig. 3 – Fig. 5 and l. 538-539, l. 554-555, l. 570-571).

4) Line 474-475; in addition to putting standard weights of axolotl at the different developmental ranges, also indicate the average length of the animals (snout to tail tip), which is the standard way that many refer to axolotl size.

We have added indications of length (snout to tail tip) and sexual maturity of animals. We believe that referring to length when describing the sizes of axolotls is slightly imprecise since this measure is highly dependable on the feeding status of the animal, but it is correct that length is often referred to in the literature when describing size, so we have included it in the manuscript nonetheless (l. 143-144 and l. 463-467).

5) Since this work is performed on vertebrate animals, some statement of ethical conduct of research (ex. IACUC approval, or approval from another regulatory agency) should be indicated.

We have added an Ethics statement section after the Acknowledgements and Disclosures with the relevant ethical approval (l. 777-780).

**Reviewer #4:**

Manuscript Summary:

This manuscript describes a protocol for study of cardiac function in an organism capable of organ regeneration. This is a very useful protocol since it gives the field a way to measure the regeneration of function whereas so far we often only observe regeneration of structure and pattern. This manuscript is highly recommended.

Major Concerns:

I have no major concerns.

Minor Concerns:

I have only 3 minor concerns which involve simple clarifications in the text.

1. It is standard in the axolotl field to describe the size of axolotls based on length in centimeters (cm) and maturity stage (larva, juvenile, sexually mature adult). This protocol uses grams (>20g, <20g). It would be useful for the field if the authors state somewhere in the manuscript the general stage and size of a 20g axolotl (sexually mature adult? 12-14 cm?).

We have added indications of length (snout to tail tip) and sexual maturity of animals. We believe that referring to length when describing the sizes of axolotls is slightly imprecise since this measure is highly dependable on the feeding status of the animal, but it is correct that length is often referred to in the literature when describing size, so we have included it in the manuscript nonetheless (l. 143-144 and l. 463-467).

2. Although most axolotl research is done on white axolotls (leucistic), the manuscript would be more useful if the authors added a sentence describing the strains of axolotls available (wildtype, melanoid, white, albino, transgenic white with GFP) and which strains would be compatible with this echocardiography protocol. Can the more darkly colored wildtype or melanoid strains be used with this procedure or does it have to be altered?

The protocol is compatible with all different strains of axolotls. We have added a sentence stating this in the introduction (l. 83-86).

3. The authors should spell out the full name and common name for MS222 somewhere in the protocol (Ethyl 3-aminobenzoate methanesulfonate, also known as 'tricane').

Full chemical names of the three anesthetics have been spelled out in the protocol (l. 107, l. 111-112, l. 115)

**Reviewer #5:**

Manuscript Summary:

This manuscript demonstrates methods for assaying cardiac function in axolotls. It will be of interest to researchers using axolotls to study physiology of the heart and, more likely, those studying heart regeneration. Developing tools for assaying regenerative function while the animal is alive is important to advance the field and should result in more researchers assaying cardiac function over the course of regeneration, which could potentially improve our understanding of how the process occurs.

Major Concerns:

none

Minor Concerns:

Are the anesthetic solutions buffered? Do they need to be checked for pH and adjusted before use? There are a few grammatical errors and syntax errors that should be caught by the in-house editor.

We are aware that some anesthesia protocols pay detailed attention to adjustments of small variations in pH, especially after reuse of the same anesthesia solution on multiple animals, however in our experience this does not have any practical implications on axolotl wellbeing and physiology if each solution is only used once, so we have left out a complicating discussion on this from the manuscript.